UNLIMITED
UNCLASSIFIED

Canada

NEW TRANSONIC TEST SECTIONS FOR THE NAE 5FTx5FT TRISONIC WIND TUNNEL

by

L.H. Ohman, D. Brown, Y.Y. Chan,
R.D. Galway, S.M. Hashim, M. Khalid,
A. Malek, M. Mokry, N. Tang, J. Thain

National Aeronautical Establishment

AERONAUTICAL NOTE
NAE-AN-62
NRC NO. 31216

OTTAWA
JANUARY 1990

National Research Council Canada
Conseil national de recherches Canada

NATIONAL AERONAUTICAL ESTABLISHMENT

SCIENTIFIC AND TECHNICAL PUBLICATIONS

AERONAUTICAL REPORTS

Aeronautical Reports (LR): Scientific and technical information pertaining to aeronautics considered important, complete, and a lasting contribution to existing knowledge.

Mechanical Engineering Reports (MS): Scientific and technical information pertaining to investigations outside aeronautics considered important, complete, and a lasting contribution to existing knowledge.

AERONAUTICAL NOTES (AN): Information less broad in scope but nevertheless of importance as a contribution to existing knowledge.

LABORATORY TECHNICAL REPORTS (LTR): Information receiving limited distribution because of preliminary data, security classification, proprietary, or other reaons.

Details on the availability of these publications may be obtained from:

Graphics Section,
National Research Council Canada,
National Aeronautical Establishment,
Bldg. M-16, Room 204,
Montreal Road,
Ottawa, Ontario
K1A 0R6

ÉTABLISSEMENT NATIONAL D'AÉRONAUTIQUE

PUBLICATIONS SCIENTIFIQUES ET TECHNIQUES

RAPPORTS D'AÉRONAUTIQUE

Rapports d'aéronautique (LR): Informations scientifiques et techniques touchant l'aéronautique jugées importantes, complètes et durables en termes de contribution aux connaissances actuelles.

Rapports de génie mécanique (MS): Informations scientifiques et techniques sur la recherche externe à l'aéronautique jugées importantes, complètes et durables en termes de contribution aux connaissances actuelles.

CAHIERS D'AÉRONAUTIQUE (AN): Informations de moindre portée mais importantes en termes d'accroissement des connaissances.

RAPPORTS TECHNIQUES DE LABORATOIRE (LTR): Informations peu disséminées pour des raisons d'usage secret, de droit de propriété ou autres ou parce qu'elles constituent des données préliminaires.

Les publications ci-dessus peuvent être obtenues à l'adresse suivante:

Section des graphiques,
Conseil national de recherches Canada,
Établissement national d'aéronautique,
Im. M-16, pièce 204,
Chemin de Montréal,
Ottawa (Ontario)
K1A 0R6

UNLIMITED
UNCLASSIFIED

NEW TRANSONIC TEST SECTIONS FOR THE NAE 5FTx5FT TRISONIC WIND TUNNEL

NOUVELLES VEINES D'ESSAI TRANSSONIQUES POUR LA SOUFFLERIE TRISONIQUE DE 5 pi SUR 5 pi DE L'ÉNA

by/par

L.H. Ohman, D. Brown, Y.Y. Chan, R.D. Galway, S.M. Hashim, M. Khalid, A. Malek, M. Mokry, N. Tang, J. Thain

**National Aeronautical Establishment/
Établissement national d'aéronautique**

**AERONAUTICAL NOTE
NAE-AN-62
NRC NO. 31216**

**OTTAWA
JANUARY 1990**

Also published in Canadian Aeronautics and Space Institute, First Canadian Symposium on Aerodynamics, December 4-5, 1989.

**Y.Y. Chan, Head/Chef
High Speed Aedrodynamics Laboratory/
Laboratoire d'aérodymique à hautes vitesses**

**G.F. Marsters
Director/directeur**

ABSTRACT

The NAE 5ftx5ft blowdown wind tunnel has undergone a major upgrade of its transonic testing capabilities. Two entirely new test sections, one for testing two-dimensional models (2D) and one for testing three-dimensional models and reflection plane models (3D), have been constructed. The two test sections are parts of the so-called Roll-in Roll-out Test Section System, so designed that an interchange between the two sections can be carried out within two days, a process that previously required about three weeks. The new test sections have, as before, perforated walls, but with different hole geometry, viz. slanted holes with splitter plates as opposed to normal holes in the original test sections. The design and manufacturing was carried out by Canadian companies.

The two test sections have been calibrated with regard to pressure distributions, flow quality (turbulence and pressure fluctuations), side wall boundary layer characteristics (2D), flow angularity and wall interference characteristics. Results from these investigations are presented and compared with corresponding data obtained in the original test sections.

RÉSUMÉ

Les capacités de la soufflerie à rafales de 5 pi sur 5 pi de l'ÉNA ont été considérablement améliorées pour les essais transsoniques. Deux veines d'essai entièrement nouvelles ont été construites, l'une pour les maquettes bidimensionnelles (2D) et l'autre pour les maquettes tridimensionnelles et les demi-maquettes (3D). Ces deux veines d'essai constituent des parties du système à veines d'essai mobiles sur rails, ainsi désigné parce qu'il permet d'interchanger les veines en moins de deux jours, un processus qui exigeait auparavant environ trois semaines. Les nouvelles veines ont, comme les anciennes, des parois perforées, mais présentent des trous d'une géométrie différente, c'est-à-dire des trous obliques avec plaques séparatrices, au lieu des trous normaux des veines d'essai originales. La conception et la fabrication de ces veines ont été confiées à des entreprises canadiennes.

Les deux veines d'essai ont été étalonnées quant à la répartition des pressions, à la qualité de l'écoulement (fluctuations de la turbulence et de la pression), aux caractéristiques de la couche limite aux parois latérales (2D) et aux caractéristiques d'angularité de l'écoulement et d'interférence des parois. Les résultats de ces études sont présentés et comparés aux données correspondantes obtenues avec les veines d'essai originales.

TABLE OF CONTENTS

TABLE OF CONTENTS (Cont'd)

LIST OF TABLES

LIST OF FIGURES

TABLE OF CONTENTS (Cont'd)

LIST OF FIGURES (Cont'd)

NOMENCLATURE

A, B, m,	constants in hot wire equation, eq.(1)
B	also width of 2D test section, 15"
c	reference length: 2D, airfoil chord, 9" 3D, mean aerod. chord, 2.982"
$C_D = \frac{\text{drag force}}{q*S}$	drag coefficient
$C_L = \frac{\text{lift force}}{q*S}$	lift coefficient
$C_N = \frac{\text{normal force}}{q*S}$	normal force coefficient
$C_p = \frac{P-P_{ref}}{q}$	pressure coefficient
M	Mach number
M_{nom}	nominal Mach number
M_{ref}	reference Mach number
$M_{\infty T}$	test section free stream Mach number
$M_{\infty c}$	$M_{\infty T}$ corrected for wall interference
M_{loc}	local Mach number
$\Delta M = M_{\infty c} - M_{\infty T}$	Mach number correction due to wall interference
P	local static pressure
P_{ref}	reference static pressure: 2D, P_{45R} 3D, P_{3DR}
P_o	stagnation pressure
$q = \frac{1}{2}\rho U^2$	free stream dynamic pressure
Re	unit Reynolds number, ft^{-1}
Rec	chord Reynolds number
S	reference area: 2D, 135 in^2 3D, 45.106 in^2
U	free stream mean velocity
u	instantaneous stream velocity
v	sidewall suction velocity
V	voltage, hot wire
V_T	tare voltage, hot wire

x	streamwise coordinate; origin 2D, balance centre-line 3D, pitch centre of rotation
y	lateral coordinate: origin 2D, south side-wall
α	angle of attack
α_g	angle between model chord plane and wind tunnel centre-line
α_c	angle of attack corrected for wall interference
α_o	flow angularity correction, +ve for floor to ceiling flow
$\Delta\alpha=\alpha_c-\alpha_g-\alpha_o$	angle of attack correction due to wall interference
ρ	free stream mean density, also instantaneous density
$\delta M/\delta x$	Mach number gradient
$\delta\alpha/\delta x$	angle of attack gradient
$\bar{}$	above quantity denotes mean value
$\tilde{}$	above quantity denotes fluctuating value

1 INTRODUCTION

AT the 1985 CASI annual general meeting in Montreal a paper was presented entitled "Recent Improvements to the NAE 5Ftx5Ft Blowdown Wind Tunnel" (Ref.1), in which certain projections were made about further enhancements of the facility. One of these projections was the incorporation of the Roll-in Roll-out Test Section System, Fig.1, and this has now been achieved. The major components of this system are a two-dimensional (2D) test section, a three-dimensional (3D) test section, both transonic, a transporter, a parking area and the original transonic plenum chamber. With this system a change in mode of operation, that is from 3D to 2D for instance, can be effected within two days, while with the "old" system such a mode change would take about three weeks. Furthermore, the walls in the new test sections are of a new design, having perforations with slanted holes with splitter plate and provision for variable porosity from 6% to 0.5%. The original perforated walls had normal holes and a fixed porosity of 20.5%

The decision to change the porosity scheme was based on a comprehensive survey of transonic wall configurations conducted by the NAE. A perforated wall was favoured over a slotted wall because of the former's much more favourable interference characteristics at sonic speed and above. The capability to reduce the porosity further enhances the wall interference characteristics at these speeds. The addition of a streamwise splitter plate in each hole eliminates the strong edge tones that are otherwise generated from perforated walls (Ref.2). The remaining wall noise is then basically that generated by the wall boundary layer. Furthermore, the wall boundary conditions in the form of pressure data, required for wall interference calculations are more readily determined for a perforated wall than for a slotted wall. Although there seems to be a consensus within the wind tunnel test community that at subsonic speed the slotted wall is more suitable, the NAE experience with their old perforated walls has shown such walls to be perfectly acceptable for subsonic testing. A third alternative, the adaptive wall, was not considered a viable alternative for a production facility like the NAE wind tunnel. Because of its complexity and mode of operation (wall contour adjustment required for each data point) the adaptive wall is more suitable for a continuous flow facility.

Being a practically 100% Canadian venture, pertinent details are presented on some of the intricacies of the design and manufacturing of the various components and the interactions between NAE, Supply and Services Canada (SSC) and Canadian industry. After a description of the system as a whole and its various components, the aerodynamic performance of the new test sections is discussed. Results are presented, covering empty tunnel pressure distributions, free stream acoustics and turbulence, side wall boundary layer characteristics

(2D test section) and wall interference characteristics. Comparisons are made with corresponding data from the original test sections.

2 DESIGN PHASE

In 1981 the NAE/NRC contracted via SSC with DSMA International Inc., Toronto, to carry out a preliminary engineering study on a system for easily interchangeable test sections for the NAE 5ftx5ft blowdown wind tunnel. The outcome of this study demonstrated that such a system, here called the Roll-in Roll-out Test Section System, was indeed viable from both a technical and an economical point of view, (Ref.3). The system would comprise a completely new 3D test section insert, a 2D test section insert that incorporated the existing 2D sidewalls, a transporter, a building annex and the existing plenum chamber. The transporter would be used to transport one insert from, say, the plenum chamber to an allocated parking space in the annex and then return with the other insert and inject it into the plenum chamber. Both inserts would have new perforated walls with 0.5" diameter holes with the axes inclined 60 degrees from the normal to the wall and facing upstream. The number of holes would be based on the requirement for 6% porosity. It was also estimated that a job of this magnitude would take about 20 months to complete at a cost of about $2 million.

The next logical step was to proceed with the final detail design, but, because of circumstances beyond NRC control, this work could not be initiated until late 1985. Again, DSMA International Inc. was awarded the contract for the final design through SSC. This design phase was completed in April 1986. An important change from the preliminary design was to include a variable porosity scheme for the perforated walls, Fig. 2. This would be accomplished by a set of sliding throttle plates mounted on the plenum side of the perforated walls. The throttle plates would have a matching set of holes. The porosity would be variable from 6% to 0.5% as determined by the position of the throttle plates. Another important new design feature was that each hole in the wall plates would have a "splitter plate", that is a thin plate that splits the hole in the middle in the streamwise direction (Ref.2). The purpose of this plate is to eliminate the strong edgetones that are generated when air passes over a sharp edge hole. These edgetones are major contributors to the overall noise level in transonic wind tunnels with perforated walls.

Other details included in the final design were interchangeable wall units to accommodate schlieren photography and sidewall balance for half-model testing, a number of port holes for mounting cameras for the NAE optical tracking system (Ref.4) and for flow visualization photography and attachment points for a roof-mounted sting. The above applies to the 3D insert. The 2D insert would have port holes for mounting cameras for flow visualization

photography. Both inserts would have a number of rows of pressure orifices in the perforated walls, in the following referred to as integral orifices. The two inserts are portrayed in isometric view in Figures 3 and 4.

The final design also included all details for the modification to the plenum chamber, the transporter, the insert parking area and other requirements in the annex.

The design of the annex was handled as a separate contract, awarded in Oct. 1987 through NRC's Administrative Services and Program Management (ASPM) Division, with a local architectural firm, G. E. Bemi and Associates. This work was completed in May 1987. An important feature of the annex design was that it would be separated from the main wind tunnel bay by a large sound-proofed sliding door. With this door closed work could be comfortably carried out in the annex, while the wind tunnel was operating.

3 CONSTRUCTION PHASE

As for the final design, the construction of the annex was managed by NRC's ASPM Division, while all other work was contracted via SSC to DSMA International Inc. as a turnkey contract, based on a proposal submitted by the Company (Ref.5). The contract for the annex, including the installation of the rails for the transporter movement, was awarded to Taplen Construction Ltd, Ottawa, in July 1987. This work was completed in July 1988. For various reasons the contract with DSMA could not be effected until August 1987. In the meantime DSMA had explored possible sources for manufacturing, having no such facilities themselves. Of particular concern was the production of the perforated wall plates. The splitter plate requirement favoured the use of EDM (Electrical Discharge Machine) technique, since the splitter plates could then be made integral with the wall plates. From a similar undertaking in Europe DSMA had access to a possible manufacturer in Europe, but at a rather high cost. By exploring the North American scene they found a company in Windsor, Build-A-Mold Inc., that showed interest and produced a sample plate with a number of 60 degree inclined holes with splitter plates, to the satisfaction of both DSMA and NAE. A Canadian supplier was thus secured, and at a 25% price advantage over the European supplier.

Consequently, and with the agreement of SSC and NAE, DSMA contracted with Build-A-Mold Inc. for the supply of the perforated wall plates, including the throttle plates. For the remainder of the work the John T. Hepburn Ltd company, Mississauga, was selected from four possible contenders. These subcontracts were in place by the end of September 1987.

During the ensuing period progress was monitored regularly by representatives from NAE, SSC and DSMA through visits to the subcontractors and meetings. It soon became apparent that the perforated plates would become a critical item. Although a satisfactory sample plate had been produced, the slight change in operation of the EDM equipment that was necessary for burning the splitter plate holes in the large 5ftx16ft wall plates caused some entirely unexpected difficulties. Being committed to produce the plates, Build-A-Mold spared no effort in resolving the situation. In particular the electrodes had to be redesigned through a trial and error process. Eventually all problems were resolved and a satisfactory product was produced, although at a slower rate than originally anticipated. However the quality of the work was of prime concern and the consequent delay just had to be accepted. The overall schedule of the project was not significantly affected, however.

The new walls will now be described in some detail. The inner walls were produced from high strength low alloy steel plates that were ground flat to a thickness of 0.375"±0.003". The burning of the holes was done on specially designed EDM equipment feeding 19 split electrodes, thus burning 19 holes at a time. The hole diameter (minor axis of the elliptic holes) and splitter plate thickness was produced to close tolerances, .500"±0.004" and 0.040±0.004". The hole pattern is depicted in Fig. 5. The narrow strips of "no holes" are where the plate is attached to the back-up structure, which also supports the throttle plates. Before the variable porosity scheme had been decided upon, it was the intent to have a number of these strips equipped with pressure orifices. However, with the variable porosity scheme going ahead it became increasingly difficult to install orifices in these strips and it was decided to relocate them in the perforated areas. The purpose of these wall pressure orifices was to use them for wall interference pressure measurements. However, considerable uncertainty existed as to whether the proximity to the perforations would cause enough local disturbances to render these measurements useless. Provisions were therefore made for installation of the 1" diameter "static tubes" used routinely for wall pressure measurements in the original test sections (Ref.6).

The throttle plates were machined from cold rolled brass to a thickness of 0.250"±0.003" with a hole pattern identical to the steel plates, but with no splitter plates in the holes. In the installed position the throttle plates are supported along the edges and along the centre through a bolt-bushing arrangement. The positions of the throttle plates are effected manually through a number of screw-jacks. The total movement available is 0.80", which allows the porosity to be varied from 6% to 0.5%. The number of holes in the 2D test section is 877 in each of the top and bottom walls and 3508 per wall in the 3D test section.

The steel plates are given a matt black oxide treatment. As well as serving as rust protection this treatment provides a surface of low reflectivity, which is a requirement for the 3D walls. This requirement stems from the need to engage the NAE Optical Tracking System (Ref.4) in aircraft stores clearance measurements. This system uses infrared diodes as optical targets and it is therefore important that all reflections are minimized. For store clearance measurements the parent model is attached to a roof mounted sting assembly shown in Fig.6, while the store model is supported on a special articulated sting. A detailed description of the NAE stores clearance facilities can be found in (Ref.4).

Work on modification of the plenum chamber commenced in January 1989. This consisted of the removal of the original perforated walls and their support structure, the installation of an adapter frame at the upstream end for accurately locating the inserts so that they align with the exit of the upstream nozzle section, the installation of rails, an inverted V-rail and a flat rail, and four locking pins with drive for locking the downstream end of the inserts. The use of the inverted V-rail ensured positive lateral guidance of the inserts when rolled in place. The precise levelling and alignment of the rails was a most stringent requirement. Also, the bolted access hatch on top of the plenum chamber was replaced by a quick access hatch with a clamshell type lock.

The erection of the prefabricated docking stations and a mezzanine floor in the annex also began in January 1989. Each docking station has the same rail arrangement as that in the plenum chamber. Again, the precise levelling of the rails was most important, particularly for the 2D insert with its side wall balance system to be calibrated in the parked insert. A good measure of the success in the levelling is that the 15 ton inserts can be shifted back and forth by hand. As can be seen in Fig. 1 there are three docking stations, one for the 2D insert, one for the 3D insert and one for possible future development.

The control logic formed a most essential part of the work. Considerable efforts were expended by DSMA and NAE staff in ensuring the safe operation of the various elements and the integration of their controls and interlocks with the wind tunnel control logic, so that no unsafe situation could arise. A detailed description of the control system is beyond the scope of this paper.

4 DELIVERY

As already mentioned, the annex was completed as a building with all its services in July 1988. Apart from the transporter rails, which were delivered during the annex construction, delivery of major components began January 11,

1989, with the arrival of the pre-constructed parts for the docking stations and the mezzanine floor. The transporter followed a few days later. Unfortunately, it arrived in a rather unsatisfactory condition. Being transported during the winter, the roads were covered with sleet, salt and sand, that became deposited onto the inadequately protected transporter. A thorough cleaning job became necessary. Of particular concern were lead screws, gear boxes and electrical conduits. The next item to arrive was the 2D insert on March 10. This was properly protected during transport in a wooden crate and arrived in good condition. The final item, the 3D insert, was delivered on July 24 in good order. Special transport was arranged by the subcontractor for these deliveries, since each shipment weighed between 15 and 20 tons.

5 COMMISSIONING AND ACCEPTANCE

To ensure the correct matching of various components critical dimensions were checked and adjustments made where necessary. The position of the transporter and its elevation is controlled by limit switches, whose positions were fixed after satisfactory alignment was confirmed by eye. The 2D insert, although it had been carefully checked dimensionally, by the contractor and NAE staff, before delivery, required adjustments of the side walls at the upstream end. In spite of having taken all the necessary steps to ensure a "perfect" match between the upstream end of the insert side walls and the mating walls located in the wind tunnel nozzle section, the first fitment showed an unacceptable mismatch. It took a few iterations to obtain an acceptable match, that is only a downstream facing step of <0.010" and an axial gap of <0.010". (An O-ring seal between mating surfaces ensures no leakage).

The plenum chamber, in its original design, was floating on springs. At the time of its design this was thought necessary to facilitate its engagement with the rest of the tunnel circuit. With the new inserts the combined weight of the plenum plus insert was heavier than before and the springs would bottom. It was therefore decided to "freeze" the plenum chamber at the appropriate height for a smooth engagement with the tunnel circuit. This also eliminated the undesirable springing of the plenum chamber when loading and unloading the inserts.

Having fitted the 2D insert in the plenum chamber and aligned it accurately with the upstream nozzle section (within ±0.005"), the rails and the adapter frame were frozen as was the level of the plenum chamber. Because of the contractors adherence to the prescribed dimensions and tight tolerances only a minor adjustment to the wheel levels was required to bring the 3D insert in line.

The final acceptance of the system as a whole required 5 consecutive successful transfers of each insert from the parking station to the plenum chamber position and return to the parking station. For the 2D insert this acceptance test was successfully carried out on March 28 and 29. Each cycle took about one hour. The upstream end of the insert has provision for bolting the support rails for the side walls to the adapter frame. These bolts and fitted shims must be installed when operating the wind tunnel. The installation and removal of the bolts and shims add nearly three hours to a transfer cycle.

A similar acceptance test was successfully performed with the 3D insert on September 1 and 5. Again the transfer cycle took about one hour. In this case there are no bolts to install so the one hour truly represents a transfer cycle time. The acceptance of the 3D insert also required the successful interchange of a number of 4ftx4ft (approximately) sections of the side walls. These sections contain the schlieren windows, the half-model balance mount and the corresponding part of the perforated wall plate with throttle plate. These interchanges were exercised in early August and demonstrated good fitment in all cases with only very minor adjustments. A number of smaller portholes (~4"diam.) and their covers for infrared cameras used for the NAE optical tracking system were similarly checked out and found acceptable.

A change in mode of operation of the wind tunnel from, say 3D to 2D involves more than switching inserts. The most upstream 2D side wall sections must be installed in the nozzle section of the wind tunnel, the so called flow constraining walls that protect the main model support strut must be installed in the diffuser section and the model support roll drive system replaced by a slender support fairing. In addition, a number of pneumatic and electrical connections must be effected and checked out before the 2D insert is ready for operation. Two full 7.5 hour working days can be regarded as a realistic time period for switching from 3D to 2D operation. A change from 2D to 3D operation would take slightly less.

The acceptance of the Roll-in Roll-out Test Section System only concerned the "mechanics" of the system. The aerodynamic performance was entirely in the hands of NAE, since the test section wall geometry, which controls the aerodynamic performance to a significant degree, had been the choice of NAE. The aerodynamic performance will be discussed in subsequent chapters.

6 INTERACTIONS BETWEEN NAE/NRC, SSC AND CANADIAN INDUSTRY

All contracts were looked after by SSC (Science Branch, Supply and Services Canada). The initial contract for preliminary design was funded directly from the normal operating funds allocated to the NAE Division. A

request for a contract, including a Statement of Work (SOW) and a sole source justification was submitted to SSC in December 1980. By the end of January 1981 the SSC had negotiated a contract with DSMA International Inc.. The reason for the sole source justification was to avoid wasteful competitive bidding, when it was clear that DSMA was the only engineering firm in Canada with relevant expertise and experience. This work was completed in May 1981 at a cost of $43K. The main conclusion was that a roll-in roll-out test section system, including an annex, could be designed and built for about $2M in 21 months.

For various reasons no further action was taken until October 1984, when NRC made a submission to Treasury Board (TB) for the approval to proceed with final design and construction. (TB approval must be obtained for projects costing more than $1M). Approval to proceed with final design was granted in August 1985. Construction was approved in principle. Subject to the result of the final design work, another submission would have to be made to TB in order to place a contract for construction. Discussions were immediately initiated between NAE/NRC, SSC and DSMA staff to lay the ground work for contract negotiations. By the end of October 1985 SSC had most expeditiously concluded a contract with DSMA for the final design.

Throughout the design process regular meetings were held between NAE and DSMA project staff and the SSC procurement officer to follow the progress and discuss various aspects of the design, making sure that NAE requirements were met. A major milestone was reached in mid January 1986 when a Project Design Review (PDR) was held. The purpose of this review was to "freeze" the design so that the contractor could start work on final production drawings. The work was completed in April 1986 at a contract price of $220K. The final design report (Ref.7) included cost and time estimates for the construction and installation of all components, excluding the annex building. The construction cost was $1.675M and the construction time 27 months. To the cost would have to be added cost for contract and construction management, warranty and risk, should the work be contracted as a turnkey supply. Due to the acute staff shortage this would be the route NAE would have to follow.

Following receipt of the final design report and production drawings and a thorough review of the same and the overall project, a submission was made in early June 1986 to TB for approval to proceed with the construction phase. The seal of approval was granted July 23, 1986 for a total expenditure of $3.685M for the overall project. This sum included costs already incurred for the design and the projected cost of the annex.

With the approval in hand NAE and SSC could enter into contract negotiations with DSMA (sole sourcing was still considered the only viable option for the same reason as for the design), but once agreement on a final

contract had been reached, it would still require the approval of TB. Contract for the annex construction could be proceeded with directly, since it was expected to cost well below $1M. Consequently a contract for the architectural design of the annex was raised by the NRC ASPM Division with G. E. Bemi and Associates of Ottawa in October 1986. This work was completed in May 1987. A contract for the annex construction was awarded to Taplen Construction Ltd of Ottawa in July 1987. A competitive bidding process was followed in awarding these contracts.

In August 1986 NRC issued a requisition to SSC to enter into negotiations with DSMA. Because of the non-competitive situation SSC was obliged to follow a fairly complex and time consuming procedure before a contract could be issued. This involved presentation of the case to a Procurement Review Committee. With the record of their favourable decision a procurement plan was prepared by the contracting officer for approval by the SSC Minister. Following that, DSMA was requested by letter in November 1986 to submit a turnkey proposal, which they did in late December 1986 (Ref.5). The technical aspect of the proposal was well in line with the NAE requirements and needed only minor modifications before being acceptable to NAE. The financial aspect was a matter for SSC to settle with DSMA. It took some rather protracted negotiations between the two parties to come to an agreement on the rate structure, overhead and profit. Furthermore, before the final contract documents could be submitted to TB for approval, they had to be reviewed by the Quality Assurance Branch of SSC.

In July 1987 the case was put before TB and approval obtained. A contract with DSMA was issued in August 1987 for the firm price of $2.435M, which was later increased to $2.500M to account for some additional work that had not been foreseen in the original contract. The closing date of the contract was to have been April 20,1989, but due to the late delivery and fitment of the 3D insert this date was amended to October 27,1989.

During the construction phase the NAE project management staff and the SSC contracting officer made frequent visits to the DSMA subcontractors Build-A-Mold, Windsor, and John T. Hepburn, Mississauga, with the DSMA project manager. The purpose of these visits was not only to follow the progress but also to make sure that the quality of workmanship conformed to the high standard required by NAE. Milestone inspections were particularly important, since an approval would allow corresponding payments to be made to DSMA and, in turn, to their subcontractors.

In conclusion this project was completed within cost but required a six month extension, from 20 to 26 months for completion. However, the fact that the 2D insert was delivered on time and the wind tunnel back in full operation in its 2D mode in May 1989, meant that the delay in the delivery of the 3D

insert had only a minor impact on the wind tunnel operation. To allow for site construction and associated NAE work the wind tunnel operations were shut down for a period of five months.

It should be mentioned that a project of this size and complexity encounters a few surprises along its path, that must be ironed out between all parties concerned. Production techniques must be changed, concessions made, schedules altered, milestones shifted around and, not the least, the paper work kept up-to-date. All through this the full understanding and trust between all parties have been essential as has the allowance for some flexibility. The division of responsibility between NAE and SSC, with NAE looking after technical matters and SSC contractual matters has worked out extremely well to the benefit of the project. The competence of the main contractor and his subcontractors has also played an important role in the successful completion of this project.

7 CALIBRATION OF THE 2D TEST SECTION

7.1 PREPARATIONS

The sidewall balances were first installed and calibrated directly in the insert. This was a departure from previous procedure, where the balances and corresponding wall sections were installed in a special calibration rig for calibration. The new set-up meant a considerable time saving from an operational point of view. The calibration results were in good agreement with earlier data.

For the static pressure calibration the following installations were made and/or checked out:

- a centre line mounted static pressure probe, Ø1.25" .
- static pressure tubes, Ø1", one each along the floor and ceiling.
- static pressure orifices integral with the floor and ceiling.
- static pressure orifices on the centre line of the north sidewall.
- a reference pressure orifice referred to as P_{45R}, on the north sidewall and 81" upstream of the sidewall balance centre-line.
- a plenum chamber pressure orifice.

All static pressure orifices were connected to scanivalves instrumented with differential pressure transducers (Kulite), with P_{45R} connected to the reference side. P_{45R} was also connected to an absolute pressure transducer (Digiquartz). A schematic of the static pressure calibration arrangements is given in Fig.7.

Other requirements were for transient wall loads, total pressure survey, sidewall boundary layer characteristics, flow quality (turbulence and acoustics), flow angularity and wall interference characteristics.

7.1.1 Transient wall loads

A fast response differential pressure transducer was installed on the north sidewall immediately after the 2D contraction, with the reference side open to the plenum chamber. The transducer would measure the pressure difference across the wall, expected to have its maximum during tunnel start-up.

7.1.2 Total pressure survey

The pitot probe rake normally used for wake drag measurements was prepared for this survey. The four pitot probes, located at spanwise stations y/B= 0.5, 0.383, 0.267 and 0.150 measured from the south sidewall, were connected to differential pressure transducers with the reference side connected to a pitot probe located at the entrance of the 2D contraction. The streamwise location of the rake was 21" downstream of the balance centreline, with a vertical traverse of 30" available.

7.1.3 Sidewall boundary layer

Two boundary layer rakes, nominally 2" and 3" in height, were mounted on the north and south sidewalls respectively at the balance centreline. Each rake had 20 pitot tubes suitably spaced and connected to scanivalves equipped with 200 psi absolute pressure transducers.

7.1.4 Flow quality

Four single element hot wire probes (0.0003"diam. tungsten wire) to be operated as constant temperature anemometers, were mounted on a common blade for installation on the south wall balance centreline. The spanwise probe locations were y/B= 0.560, 0.440, 0.323 and 0.207, measured from the south sidewall. To complement the hot wire measurements a microphone probe (0.125" diameter B&K condenser microphone) was installed on the centre plane of the insert close to the balance centre-line and 7.5" above it. Furthermore, a flush mounted fast response pressure transducer was installed on the north sidewall 30" upstream of the balance centreline. For measuring total head fluctuations a fast response pitot probe was mounted on the south sidewall about half way between the hot wire probe and the ceiling. The frequency response of the pressure instrumentation was flat for frequencies up to at least 15 kHz. RMS meters required to obtain direct readings of the rms values of the various sensors had a bandwidth from 30Hz to 20kHz and a time constant of 0.25 second. All signals were also to be recorded on FM-tape. The overall arrangement of the flow quality measurements is depicted in Fig.8.

7.1.5 Flow angularity and wall interference characteristics

Using a 9" chord supercritical airfoil model the flow angularity would be determined from measured balance forces over a small incidence range, with the model in upright and inverted position. The same model would be used, in its upright position, to determine the wall interference characteristics. In addition to measuring model forces and pressures, wall pressure data from the static tubes and the integral pressure orifices would be obtained over an extended incidence range. The data thus collected would then be analyzed using the wall interference method developed by Mokry (Ref.6).

7.2 RESULTS

7.2.1 Static pressure calibration

Measurements were performed in the Mach number range 0.12 to 0.85 at Reynolds numbers 6×10^6 to 24×10^6 per foot and at 6%, 4% and 2% wall porosity. Some typical results are shown in Fig.9 in the form of $M_{loc}-M_{ref}$, with M_{ref} being a reference Mach number measured at a station on the north sidewall located 5.4 tunnel widths (81") upstream of the balance centre-line. Note that data from three repeat pressure scans are shown. The centreline probe and the floor and ceiling static tube data are in good agreement, demonstrating a uniform flow through the test section. The repeatability is very good. A negative Mach number gradient, or, a positive pressure gradient is prevalent. For the 6% and 4% porosity cases the gradient is quite pronounced at the most downstream part of the test section. The north sidewall pressure data, not shown, show consistently slightly higher adverse pressure gradient than the centreline and the floor and ceiling data. This is rather puzzling, since in the original 2D insert, using the same sidewalls and centreline probe, no such discrepancy was observed (Ref.8). No satisfactory explanation can be offered for this discrepancy.

Because of the large amount of data collected in this phase of the calibration it is convenient to quantify the data to yield the following:

test section free stream Mach number $M_{\infty T}$

test section streamwise Mach number gradient $\delta M/\delta x$ in^{-1}

The two quantities are determined from a least squares fit of the experimental data for $-1<x/B<1$. To obtain a measure of the spread of data the standard deviation is computed.

$$\sigma = \left[\frac{\sum_{1}^{N}(y_i - \bar{y}_i)^2}{N - 1} \right]^{1/2} \qquad \text{for } -1<x/B<1$$

where y_i is a measured value and $\bar{y}_i$ the corresponding (for same x) straight line fit value.

The results of this analysis of the data are presented in Table 1 for a number of wind tunnel runs. Only the analysis of the first pressure scan data of the three scans performed for each wind tunnel run is presented, since the repeatability between scans was found to be very good. Neither the gradient nor the standard deviation show any particular trend with Mach number or porosity. Although the small negative Mach number gradient may seem undesirable, it should be kept in mind that the presence of a model and its wake alters the gradient, due to wall interference effects, under some conditions reducing it or even changing its sign.

The data obtained from the integral orifices in the floor and ceiling, see Figure 9b, show large but repeatable excursions between adjacent orifices at all porosities. The local effect of the flow through the individual slanted holes is believed to be the cause of this irregularity and makes it doubtful that the integral orifices can be used for boundary measurements required for wall interference assessment.

7.2.2 Transient wall loads

There were some concerns that the transient wall loads during tunnel start-up at low porosities might be on the high side compared with the loads measured at 20.5% porosity for the original 2D insert (Ref.9). However the present measurements alleviated these concerns. Pressure data across the north sidewall were obtained for Mach numbers from 0.12 to 0.85, stagnation pressures from 34 to 120 psia and wall porosities from 6% to 2%. The maximum pressure differential was obtained for M=0.85, P_o =120 psia and 4% porosity and measured -10.5 psi (higher pressure in the plenum chamber). This value is comparable in magnitude to the 12 psi measured with the 20.5% porosity walls at M~1 and P_o=118psia (Ref.9). The pressure signatures for the two cases, however, look quite different, Fig.10. The present data show both a positive and a negative peak, with the negative peak in this case having the larger value, while the earlier data only show a positive peak. The reason for the different pressure signatures are believed to be mainly due to the difference in the structure of the two arrangements. The original 2D test section was assembled inside the 5ftx5ft 3D test section that was integral with the plenum chamber, while the roll-in roll-out 2D section is a self-contained unit installed in an empty plenum chamber.

7.2.3 Total pressure survey

The survey was conducted at four discrete lateral stations from 2.25 to 7.5 inches from the south sidewall in a vertical plane 21" downstream of the

balance centre-line. The vertical excursion was from 8" below the centre-line to 18" above. Results were obtained at M=0.5 and 0.75 and they show a very uniform distribution. In general the variations observed are less than 0.1 psi, even for stagnation pressures as high as 107 psia, which is largely within the measurement accuracy.

7.2.4 Sidewall boundary layer characteristics

The sidewalls in the roll-in roll-out insert are the same as for the original 2D facility. However, they had been refinished and sanded to a good surface finish, ~32 μin, in order to obtain as thin a boundary layer as possible. Measurements were made with the boundary layer rakes at various conditions with and without sidewall suction. Representative results are depicted in Fig.11 in the form of displacement thickness versus Reynolds number and suction respectively. Data from measurements in the original 2D test section are also shown. The 1983 results were obtained with the sidewalls in their original condition (apart from wear and tear) with a very smooth suction surface (60 μin). Due to local flaking of the suction surface, the suction panels were replaced by a coarser (about 600 μin) material in 1984, which is reflected in the 1984 data. Although these same suction panels apply to the present data, the effect of improved surface finish upstream of the suction area has resulted in a boundary layer thickness thinner than that measured in both 1983 and 1984.

A thin sidewall boundary layer is crucial to the success of establishing good two-dimensional flow over airfoil models. Furthermore, a correction to the test Mach number based on the thickness of the boundary layer relative to the tunnel width is considered important by some researchers (Ref.10). When applying this correction, the boundary layer shape factor enters the calculations as a parameter. Present and previous data give a shape factor value of ~1.5±0.05, with no discernible effect of Reynolds number and a very weak reducing effect of suction.

7.2.5 Flow quality

Hot wire and high frequency pressure fluctuation measurements were carried out at Mach numbers from 0.4 to 0.8 and at Reynolds numbers from 6×10^6 to 35×10^6 per foot. In order to emulate conditions during model testing sidewall suction was applied throughout this investigation, nominally 0.8% ratio of suction velocity over free stream velocity. The hot wire data were processed to yield mass flux fluctuations, $\widetilde{\rho u}$, and, in combination with the centreline microphone data, an estimate of the turbulence intensity, $\widetilde{u}/\overline{u}$. In evaluating the hot wire data it is assumed that the temperature fluctuations are negligible and that the relation between heat loss and mass flux can be expressed as (see Ref.11, e.g.)

$$\frac{i^2 R}{R - R_o} = A + B(\rho u)^m \qquad (1)$$

a form similar to the often referred to King's equation. For constant temperature anemometry R is constant and, by substituting the voltage V across the wire for iR, this equation can be rewritten as

$$V^2 = A + B(\rho u)^m \qquad (2)$$

or

$$(\bar{V} + \tilde{V})^2 = A + B(\overline{\rho u} + \widetilde{\rho u})^m \qquad (3)$$

By series expansion of the bracketed terms and ignoring second order quantities eq. (3) can be approximated by

$$\bar{V}^2 + 2\bar{V}\tilde{V} = A + B\overline{\rho u}^m(1 + \widetilde{\rho u}/\overline{\rho u}) \qquad (4)$$

The constants A and B are determined as follows. For zero mass flux, $\rho u=0$, eq. (2) gives

$$A = V^2 = V_T^2$$

The constant B is obtained from eq. (3), assuming steady flow, as

$$B = (\bar{V}^2 - V_T 2)/\overline{\rho u}^m$$

The exponent m was determined from log plots of $\bar{V}^2 - V_T^2$ vs ρu and found to vary between 0.44 and 0.62, with the value generally decreasing with increasing mass flux, but with hardly any discernible effect of Mach number. For the processing of the present data a constant value of $m=0.5$ has been used. Thus substituting for the constants A, B and m, as described above, in eq(4) and rearranging the terms, we arrive at

$$\widetilde{\rho u}/\overline{\rho u} = 4\bar{V}\tilde{V}/(\bar{V}^2 - V_T^2) \qquad (5)$$

For the quantity of interest, $(\widetilde{\rho u}/\overline{\rho u})_{rms}$, we then have

$$(\widetilde{\rho u}/\overline{\rho u})_{rms} = \frac{4(\tilde{V}/\bar{V})_{rms}}{1 - V_T^2/\bar{V}^2} \qquad (6)$$

which is the expression used to evaluate the hot wire signals.

To obtain the velocity fluctuations u/u we follow the procedure of Ref.12, combining the mass flux data with the microphone data according to

$$\left(\widetilde{u}/\overline{u}\right)_{rms}^{2} = \frac{\left(\widetilde{\rho u}/\overline{\rho u}\right)_{rms}^{2} + \left(\widetilde{p}/\overline{p}\right)_{rms}^{2}}{\left[1 + (\gamma-1)M^{2}\right]^{2}} \qquad (7)$$

where $\widetilde{p}/\overline{p}$ is the pressure fluctuations measured by the microphone normalized by the free stream mean static pressure.

Early in the investigation a problem developed with the No 1, central, wire and the signal from this probe had to be discarded. During a wind tunnel run the rms value of all fluctuating signals, hot wire, microphone, total pressure and sidewall pressure, was formed over a 2.5 second period (equivalent to a pressure scanning period). Up to 20 values were obtained during one run. A summary of typical results for Mach numbers from 0.4 to 0.8 at a Reynolds number of 15×10^6 and at 2% porosity is presented in Table 2. The values given are the averages for a run, with the maximum spread between individual 'scans' indicated. To ensure that signals affected by the tunnel starting transient are excluded, only data obtained after about 8 seconds of run time are considered. The hot wire signals in particular were noticeably affected by the starting transient.

No particular trend with Mach number can be observed for the hot wire and sidewall pressure data. The microphone and total pressure data, however, show increasing values with Mach number. Although not presented, data obtained at other Reynolds numbers showed no particular trends with Reynolds number, except the total pressure fluctuations, that increased with increasing Reynolds number.

The velocity fluctuation, or turbulence intensity, $\left(\widetilde{u}/\overline{u}\right)_{rms}$, calculated according to eq.(7) is depicted in Fig.12 vs Mach number for Re= 15×10^6 per ft. The mass flux values used are the run averages for the three wires. It is interesting to note that the acoustic contributions to the turbulence intensity values dominate at the higher Mach numbers. The turbulence has a minimum of 0.23% at M=0.5 and increases to .35% at M=0.8.

The sidewall static pressure fluctuations are compared with the microphone data in Fig.13 in terms of Cp_{rms} for Re= 15×10^6. The microphone data show a slight increase with Mach number, from 0.55% at M=0.4 to 0.8% at M=0.8. The sidewall results are higher by about 0.5% to 0.8%, which is consistent with the contribution to be expected from the wall boundary layer itself (Ref.13).

Sample power spectra of the microphone and the sidewall transducer signals are shown in Fig.14. They confirm that the edgetones generated by perforated walls are effectively eliminated by the splitter plate design. In the spectrum in part (b) of the figure, obtained in the original 2D test section with 20.5% porosity and normal holes, the pronounced peak at 6.2 kHz is attributed to edgetones. This peak was eliminated in the original test section by covering the perforations with a fine mesh screen, (Ref.1). The dotted line in Fig.13 represents the upper limit of the sidewall measured Cp_{rms} in the old facility and is slightly lower than in the present test section. This is not entirely unexpected. Vaucheret has shown (Ref.14) that the fine mesh technique actually reduces the noise even more effectively than the splitter plate technique. In practice, however, it is very difficult to apply the fine mesh screen to a large surface in a blowdown wind tunnel and maintain the structural integrity of the screen. Another reason for the higher noise level is the higher outflow from the plenum chamber into the diffuser due to the higher plenum chamber pressure, a consequence of the slanted holes. The increased noise from the more intense mixing in the diffuser re-entry area would be transmitted upstream and sensed by the pressure instrumentation. With the original perforated walls the plenum pressure was always slightly lower than the test section static pressure and, as a consequence, very little, if any, outflow would occur from the plenum chamber into the diffuser.

Of interest also is to compare the absolute rms-level of fluctuations of the free stream static pressure measured by the microphone and of the total pressure measured by the pitot tube in the test section, Fig.15. Both levels increase in unison with increasing Mach number, with the total pressure values being about 0.03 to 0.04 psi higher than the static pressure values. The power spectra shown on the figure demonstrate very similar characteristics for the two pressures, with a pronounced peak at about 400 Hz. The origin of this peak is at present unknown. It seems reasonable to deduce that the total pressure fluctuations are the major source for the static pressure fluctuations.

7.2.6 Flow angularity

This was determined at the model location only from balance measurements with the model in upright and inverted position. This part of the calibration was limited to a few test conditions only for 4%, 3% and 2% porosity. The results are plotted in Fig.16 and show a maximum upwash of <0.17 degree. The only parameters having a noticeable effect are Mach number, and to a lesser degree wall porosity. Stagnation pressure and control valve position have no discernible effect. No attempt has been made to find the source of this flow angularity, which is slightly higher than for the old facility, <0.07 degree downwash.

7.2.7 Wall interference characteristics

These have been evaluated by the method of Mokry, Ref.6, applied to a series of measurements of floor and ceiling pressure distributions in combination with model force measurements. Only the static pressure tube data have been analyzed, the data obtained from the integral pressure orifices were considered unsuitable, as previously explained. As a measure of wall interference the corrections to free stream Mach number, angle of attack and their respective streamwise gradients, at the model location are used.

Figures 17 and 18 show the corrections to Mach number and angle of attack respectively against the normal force coefficient for nominal Mach numbers from 0.5 to 0.8 for 2% wall porosity. Also depicted are corresponding data from an earlier investigation in the 20.5% porosity test section, (Ref.15). The lift dependency of the corrections is significantly smaller for the 2% porosity, particularly in case of the Mach number correction. At M=0.5 ΔM remains constant at -0.0025 over the full C_N-range, compared to an excursion of 0.006 for the 20.5% walls. At M=0.8 the ΔM-excursion is 0.005 for the 2% and 0.011 for the 20.5% porosity case. However, in this case the ΔM for zero lift is higher for 2% than for 20.5% porosity, 0.006 vs 0.002, due to the more pronounced solid blockage effect at the lower porosity.

The streamwise Mach number and angle-of-attack gradients are plotted in Fig.19 for the 2% and 20.5% walls. The M-gradient is quite small in both cases with hardly any Mach number dependency, less than $|0.0017|$. For the new test section the gradient has its largest value (negative) near zero lift and becomes practically zero at high lift. In the old test section the gradient remains positive for all lift values. The α-gradient shows a linear increase with lift for the present test section, while it is nearly constant and close to zero for the original test section. In the latter case the gradient was $<|0.03°|$, while for the 2% walls it reaches a maximum value of 0.162° over the 9" chord airfoil at M=0.5 and C_N=1.186. An estimate of the 0.162° cambering effect yields an increase of 0.005 in C_N, based on thin airfoil theory.

In an AGARD report on wind tunnel flow quality (Ref.16) it is recommended that the Mach number gradient should be $<0.0006M$ and the angle of attack gradient (flow curvature) <0.03°. These values are based on an accuracy requirement of 0.0001 in the drag coefficient C_D, a very stringent requirement. The 2% porosity test section meets the M-gradient requirement at higher lift, while the α-gradient criteria is met only at low lift.

The drag polars plotted in Fig.20 show generally good agreement between the two sets of data. In the low drag region the scatter between the '2%' and '20.5%' data is about 0.0001 in C_D, demonstrating no significant gradient effect in both cases. The difference observed at M=0.8 at lower lift could

possibly be a Mach number effect; the old data were obtained at a Mach number 0.001 to 0.002 lower than the present data. The dramatic difference in drag at the highest lift for M=0.5 is thought to be caused by the M-gradient (or pressure gradient), which has a favourable sign for the 20.5% data and unfavourable sign for the 2% data. When the boundary layer is close to incipient separation, as is the case near maximum lift, even a very small gradient can have a significant effect.

8 CALIBRATION OF THE 3D TEST SECTION

8.1 PREPARATIONS

For the 'empty tunnel' static pressure calibration static pressure tubes, similar to the ones used for the 2D calibration, were installed near the centre on each of the four walls and connected to scanivalves. In view of the experience with the 2D calibration, only two rows of integral pressure orifices, one on the ceiling and one on the south wall, were connected to scanivalves. A centreline mounted static pressure probe was also prepared for scanning its 36 pressure orifices. The nose of the probe was designed so that it could accommodate either a hot wire probe or a microphone. Fig.21 outlines the calibration arrangement. For a first assessment of the wall interference characteristics 6-component balance measurements with a sting-mounted swept wing model, Fig.22, were organized. The wall static pressure measuring arrangement remained as for the empty tunnel calibration. Because of the low geometric blockage of this model, 0.1%, the interference effects were expected to be very small. Separate measurements with a much larger model with about 1% geometric blockage will provide additional data at a later date. The smaller model would also be used to determine the free stream flow angularity from balance data obtained with the model in upright and inverted position.

8.2 RESULTS

8.2.1 Static pressure calibration

Measurements were performed in the Mach number range 0.2 - 1.32 at Reynolds numbers from $3x10^6$ to $13x10^6$ and at 6% to 1% wall porosity. Only results for Mach numbers up to M=1 will be discussed here. Representative Mach number distributions in the form of $M_{loc}-M_{ref}$ are depicted in Figures 23 and 24 for nominal Mach numbers 0.5 and 0.9 at 2% wall porosity. The reference Mach number M_{ref} is obtained from the local static pressure at a station located 73.5" upstream of the pitch centre of rotation, on the north wall. In order not to congest the graphs, data from two of the static tubes have been omitted. As for the 2D case data for repeat pressure scans, in this case four scans, are overplotted, showing good repeatability. The results show a uniform Mach number distribution over the uniform porosity region with a small negative gradient

over the model location area. The most down-stream part of the centre-line probe results show the adverse effect of the model (probe) support. The integral wall pressures do not show the large excursions between adjacent orifices, that was the case with corresponding data from the 2D test section. Apart from a few 'waves' they are very similar to the static tube data. It is therefore believed that the integral wall pressures will be usable for wall interference assessment.

As for the 2D case the data for a number of wind tunnel runs have been evaluated to yield the test section free stream Mach number $M_{\infty T}$, the stream-wise Mach number gradient $\delta M/\delta x$ and the standard deviation σ, using the first scan data from the centre-line probe over the 40" model location region indicated in Figures 23 and 24. The results are presented in Table 3. The only consistent trend to be seen is that the M-gradient value for 2% porosity decreases with increasing Mach number, the M=0.8 result being an exception. The M=0.9 results show increasing gradient values with increasing porosity. Both the gradients and the standard deviation values are of the same magnitude as for the 2D test section.

8.2.2 Flow quality

Hot wire and static pressure fluctuation (microphone) measurements were performed at Mach numbers from 0.2 to 0.9 for Reynolds numbers $6x10^6$ and $9.5x10^6$ and with 6%, 4% and 2% wall porosities. The data have been processed in the same way as for the 2D test section data. The microphone data are depicted in Fig.25. For M>0.5 the trend is for the noise level to increase with increasing porosity and increasing Mach number. Data obtained in the original 20.5% porosity test section (Ref.1) are also shown for comparison. This curve has a different character with a maximum at M=0.7. At this Mach number there is about 30% reduction in the noise level with the new walls at 2% porosity. The power spectra for 4% and 2% porosities in the upper part of the figure show that the major contributions to the noise are in the lower frequency domain, <1kHz, and believed coming from the mixing of the plenum chamber air with the test section air in the diffuser re-entry area. As for the 2D test section there is no sign of any edge-tones, that would otherwise have shown up as a pronounced peak in the 7 to 9 kHz range.

The mass flux and turbulence intensity data are summarized in Fig. 26. The data are presented as vertical bars, since no consistent trend with porosity was found. Both quantities show increasing values with increasing Mach number for M>0.3. As in the 2D case the contribution from the static pressure fluctuations to the turbulence intensity becomes significant at the higher Mach numbers. The turbulence has a minimum of about 0.35% at M=0.3 and increases to about 0.65% at M=0.9. No corresponding data are available for the original test section.

8.2.3 Flow angularity

This was determined from model force measurements with the model in upright and inverted position for Mach numbers from 0.6 to 1.0 at Reynolds number $8x10^6$/ft and for 4%, 2% and 1% wall porosities. The results, plotted in Fig.27, show a small downwash for all porosities, the maximum value being 0.35° at M=0.6 and 4% porosity. At the higher Mach numbers the downwash varies between 0.25° and 0.15°, with the lowest value being for 2% porosity. In general the flow angularity is about 0.1° less than for the original test section.

8.2.4 Wall interference

Measurements of model forces, with fixed transition, and wall pressure distributions were carried out in the Mach number range 0.8 to 1.1 at Reynolds number $8x10^6$ and at 6%, 4%, 2% and 1% wall porosities. The wall interference analysis is based on a method developed at NAE and described in Ref.17. The static pressure tube data were used to represent the wall boundary conditions. The method is only applicable to data for M<1 (subsonic conditions at the wall). At this stage only the zero lift data have been analyzed.

The calculated corrections ΔM to the test section Mach number have been summarized in Fig. 28. As expected, because of the small model (0.1% blockage) the corrections are small, the largest being $\Delta M = 0.0045$ for 1% porosity at M=0.98. For M<0.9 the corrections are less than 0.002. The scatter of the ΔM values are of the same magnitude, but they are always positive. Because of the scatter it can not be conclusively stated, but the trend appears to be for ΔM to increase with decreasing porosity, as would be expected for solid blockage corrections.

The zero lift drag coefficient data in Fig. 29 show good agreement between the various porosity cases, within ±5 drag counts. They are also in good agreement with data obtained in the original 20.5% porosity test section (Ref.18). No ΔM-corrections have been applied to the latter data, but because of the larger porosity it would be expected that any ΔM-correction would be smaller than for the present test section and therefore hardly discernible. For M>1 no corrections have been applied in either case and previous and present data appear to fall well in line. Although these results are not a severe test on wall interference characteristics, they demonstrate that the determination of the test section Mach number (from plenum chamber pressure in the old test section and from an upstream reference wall pressure in the new test section) is consistent in both cases.

9 CONCLUSIONS

The incorporation of the Roll-in Roll-out Test Section System represents a major upgrade of the transonic testing capabilities of the NAE 5ftx5ft trisonic wind tunnel. The various phases of the project; preliminary engineering design study, final detail design, construction and commissioning, were all carried out within cost and largely within projected time frames.

The system comprises a 2D and a 3D test section, a transporter, a parking area and the original transonic plenum chamber. A change in mode of operation from, say, 3D to 2D can be effected in two days, as opposed to the 3 weeks in the original arrangement. This represents a considerable saving in time that can be used as productive wind tunnel time.

The new variable porosity test section walls, having slanted holes with splitter plates, allow the wall porosity to be varied between 6% and 0.5% for optimizing wall interference or other flow characteristics. The old test section walls had normal holes with fixed porosity, 20.5%.

Analysis of initial calibration results of the two test sections have revealed the following characteristics:

for 2D test section for $0.4 \leq M \leq 0.85$

- good uniform flow at 6% to 2% wall porosities with a small negative stream-wise Mach number gradient, of the order of 10^{-4} in^{-1} over the model test area, with no consistent trend with either Reynolds number or porosity. The standard deviation σ_M over the same area is of the order 10^{-3}.

- at 2% porosity and $Re=15 \times 10^6$/ft the mass flux rms varies between 0.2% and 0.3% and the turbulence intensity between 0.23% and 0.35%. The acoustic contribution to the turbulence intensity becomes significant at higher Mach numbers.

- free stream flow angularity is $<0.17°$ upwash.

- the integral wall pressure data show too large irregularities to be used for wall interference assessment, the static pressure tube data are of acceptable quality for this purpose.

- wall interference effects for a 9" chord airfoil model and 2% wall porosity, in comparison with those for the old test section, show smaller Mach number and angle of attack corrections, reduced Mach

number gradients at higher lift coefficients but increased angle of attack gradients (flow curvature) at higher lift coefficients.

- drag polars obtained at 2% wall porosity are in good agreement with old test section data, except for M=0.5 near maximum lift, where the difference can be attributed to the different sign of the Mach number gradient for the two test sections and its effect on the boundary layer near incipient separation.

- a number of external client investigations have already been performed, demonstrating a preference for operating the facility at 2% to 3% wall porosity.

for 3D test section, for 0.5<M<1

- good uniform flow with a small stream-wise negative Mach number gradient of the order of 10^{-4}/in over the model test area, with no consistent trend with Reynolds number. At M=0.9 the value of the gradient increases with increasing porosity. The standard deviation σ_M over the model area is of the order 10^{-3}.

- the mass flux rms and the turbulence intensity show no consistent trend with porosity and vary from 0.3% to 0.45% and 0.3% to 0.65% respectively, with the values increasing with increasing Mach number.

- the free stream flow angularity is generally 0.1°(downwash) less than for the old test section, the maximum measured is 0.35° at M=0.6 and 4% porosity.

- the integral wall pressure data show much smaller excursions than in the 2D case and appear to be acceptable for wall interference assessment as an alternative to the static pressure tube data.

- wall interference effects, due to the small model used, are hardly discernible at all porosities, 6% to 1%. Zero lift drag data show excellent agreement with data obtained in the old test section up to M=1.1, demonstrating consistency in the way the Mach number is determined in the two cases.

The new test sections have untapped potential yet to be explored. The interference characteristics of the 3D walls need to be further examined using a bigger model. The possibility of using unequal porosity for floor and ceiling for lifting models, as discussed in Ref. 19, should be examined, particularly

in the 2D case, for which it has been shown by Williams and Parkinson (Ref.20) that a solid floor and ventilated ceiling produces near interference free flow at low speed. The Roll-in Roll-out Test Section System has so far lived up to its expectations.

ACKNOWLEDGMENTS

Special thanks are due to the DSMA project manager Mr R. Dzoja and his support staff, including sub-contractors, to the SSC procurement officer Miss M. Shaar and the support given by her department and to staff of the High Speed Aerodynamics Laboratory of NAE for the vital role they all played in the successful completion of this project.

REFERENCES

1 Ohman, L. H.
Brown, D.
Bowker, A. J.
Ellis, F. A.
Recent Improvements to the NAE 5ftx5ft Blowdown Wind Tunnel. NAE/NRC AN-31, Aug. 1984

2 Dougherty,Jr.,N. S.
Anderson, C. F.
Parker, Jr., R. L.
An Experimental Study on Suppression of Edgetones from Perforated Wind Tunnel Walls. AIAA Paper 76-50, Jan. 1976

3
Interchangeable Working Section Inserts for the NAE 5ft Trisonic Wind Tunnel. Preliminary Engineering Study. DSMA International Inc. Rept. No 4022/R42, May, 1981

4 Brown, D.
Bureau, J. L.
The NAE System for Grid Measurements of External Store's Forces. AIAA Paper 88-2064, May 1988

5
Roll-in Roll-out Test System for NAE 5ftx5ft Trisonic Wind Tunnel. Proposal for Turnkey Supply DSMA Internatinal Inc. Prop. No 961/34/P192, Dec. 1986

6 Mokry, M.
Ohman, L. H.
Application of the Fast Fourier Transform to Two-dimensional Wind Tunnel Wall Interference. AIAA J. of A. Vol.17,No 6, June 1980

7
Roll-in Roll-out Test System for NAE 5ftx5Ft Trisonic Wind Tunnel. Design Phase, Final Report. DSMA International Inc. Rept. No 4074/R168 April 1986

8 Ohman, L. H.
The NAE 15inx60in Two-dimensional Test Facility: New Features and Some Related Observations, Results of new Centre-line Calibration at 20.5% Porosity. NAE/NRC LTR-HA-15, March 1973

9 Ohman, L. H.
Brown D.
The NAE High Reynolds Number 15inx60in Two-dimensional Test Facility. NAE/NRC LTR-HA-4, Part II, Sept. 1970

10 Murthy, A. V. — Effects of Aspect Ratio and Sidewall Boundary Layer in Airfoil Testing. AIAA J. of A. Vol.25 No 3, March 1988

11 Serafini, J. S. — Wall Pressure Fluctuations and Pressure-Velocity Correlations in a Turbulent Boundary Layer. NASA TR R-165, Dec. 1963

12 Jones, G. S. Steinback, P. C. — A New Look at Wind Tunnel Flow Quality for Transonic Flow. SAE Technical Paper Series 881452 Oct 1988

13 Willmarth,W. W. — Pressure Fluctuations beneath Turbulent Boundary Layers. Annual Review of Fluid Mechanics, Vol.7,1975

14 Vaucheret, X. — Fluctuations Acoustiques Engendre'es par les Parois Permeables d'une Soufflerie Transsonic. AGARD CP-174, March 1986

15 Chan, Y. Y. — Wind Tunnel Investigation of Cast 10/DOA-2 12% Supercritical Airfoil model. NAE/NRC LTR-HA-5x5/0162, May 1986

16 Steinle, F. Stanewsky, E. — Wind Tunnel Flow Quality and Data Accuracy AGARD-AR-184, ed. by R. Dietz, Nov. 1982

17 Mokry, M. — Subsonic Wall Interference Corrections for Finite-length Test Sections Using Boundary Pressure Measurements. AGARD-CP-335, Paper No. 10, Sept.1982

18 Chan, Y. Y. Tang, N. — Private Communications, 1987

19 Mokry, M. Chan, Y.Y. Jones, D.J. — Two-Dimensional Wind Tunnel Wall Interference. AGARD-AG-281, Chapter 5, Nov. 1983

20 Williams, C. D. Parkinson, G. V. — A Low Correction Wall Configuration for Airfoil Testing. AGARD-CP-174, Paper No 21, Sept. 1975

TABLE 1

M_{nom}	Re * 10^{-6} /ft	Porosity %	$-1 \leq {}^{X}/_{B} \leq 1$ (B = 15")		
			$M_{\infty T}$	${}^{\delta M}/_{\delta X}$* 10^{4} in^{-1}	σ_M * 10^3
0.40	15	2	0.392	-0.355	0.80
0.40	15	4	0.391	-0.993	1.20
0.40	15	6	0.391	-1.520	1.70
0.70	24	2	0.686	-0.400	1.20
0.70	24	4	0.686	-0.990	1.20
0.70	24	6	0.687	-0.560	1.10
0.80*	26	2	0.802	-0.850	1.80
0.80*	26	4	0.801	-0.170	1.20
0.84	26	6	0.836	0.944	1.20
0.85*	26	2	0.856	-0.570	1.60
0.85*	35	4	0.854	-0.100	1.60

Centre-line probe data except for * indicating ceiling static tube data.

Static Pressure Calibration Results

2-D Test Section

TABLE 2

MACH No.	Mass flux			Static pressure			Total pressure
	% $(\widetilde{\rho u}/\overline{\rho u})_{rms}$			Centre-line		Sidewall	
	Probe 2	Probe 3	Probe 4	Cp_{rms} %	$(\widetilde{p}/\overline{p})_{rms}$ %	Cp_{rms} %	$\widetilde{Po}_{rms}$ psi
	$y/_B$=.44	0.323	0.207				
0.41	* 0.27 +2 -3	0.22 +3 -2	0.26 +4 +4	0.58 +3 -1	0.068	1.35 +7 -4	0.089 +6 -5
0.51	0.23 +1 -3	—	0.24 +3 -3	0.63 +1 -1	0.115	1.36 +1 -1	0.111 +1 -2
0.61	0.21 +2 -2	0.29 +1 -1	0.17 +2 -1	0.78 +2 -1	0.203	1.44 0 -1	0.135 +1 -1
0.71	0.28 +5 -2	0.29 +2 -2	0.20 +2 -2	0.82 +3 -3	0.289	1.40 +1 -2	0.149 +1 -1
0.81	0.28 +5 -2	0.29 +2 -2	0.20 +2 -2	0.77 +3 -1	0.354	1.32 +3 -2	0.151 +4 -3

* The ± figures indicate the spread in the last digit over about ten 2.5 second averaging periods.

2-D Test Section Flow quality Results

2% Porosity Re = 15 x 10^6/ft

TABLE 3

Run#	M_{nom}	Re x 10^{-6} /ft	Porosity %	$-25" \leq x \leq 15"$		
				$M_{\infty T}$	$\delta M/\delta x * 10^4$ in^{-1}	$\sigma_M * 10^3$
35045	0.50	6.0	2	0.512	-0.82	1.30
35046	0.50	9.5	2	0.512	-1.09	1.48
35047	0.50	13.0	2	0.512	-1.08	1.42
35051	0.70	6.0	2	0.718	-0.38	0.69
35052	0.70	9.5	2	0.719	-0.55	0.98
35053	0.70	13.0	2	0.720	-0.10	0.77
35054	0.80	13.0	2	0.821	-0.68	1.18
35055	0.90	9.5	2	0.923	-0.35	1.12
35056	0.90	13.0	2	0.925	-0.50	1.14
35014	0.97	10.0	2	0.987	-0.14	0.91
35057	0.90	9.0	4	0.928	-0.63	1.49
35066	0.90	9.0	6	0.942	-1.15	1.69

Centre-line Static Pressure Calibration

3-D Test Section

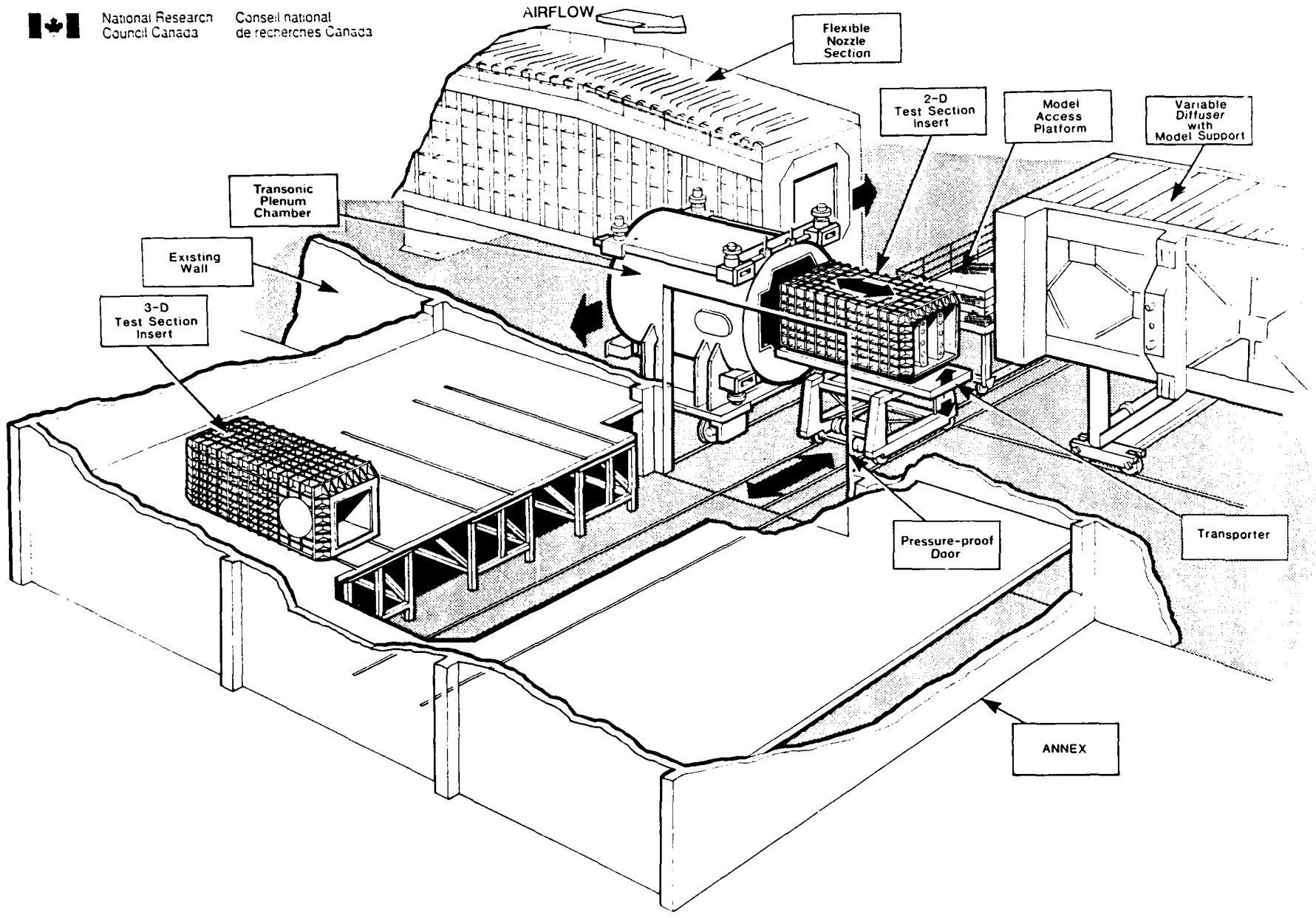

FIG. 1: ROLL-IN ROLL-OUT TEST SECTION SYSTEM, NAE 5-FT X 5-FT WIND TUNNEL

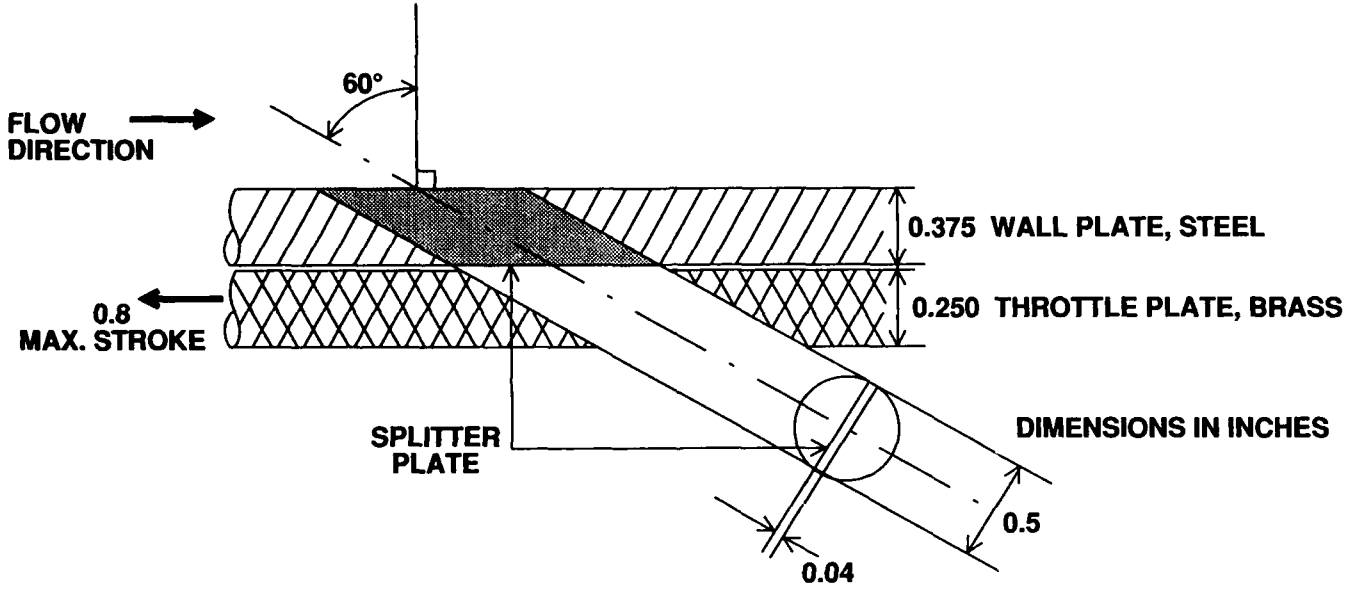

FIG. 2 VARIABLE POROSITY WALL HOLE GEOMETRY

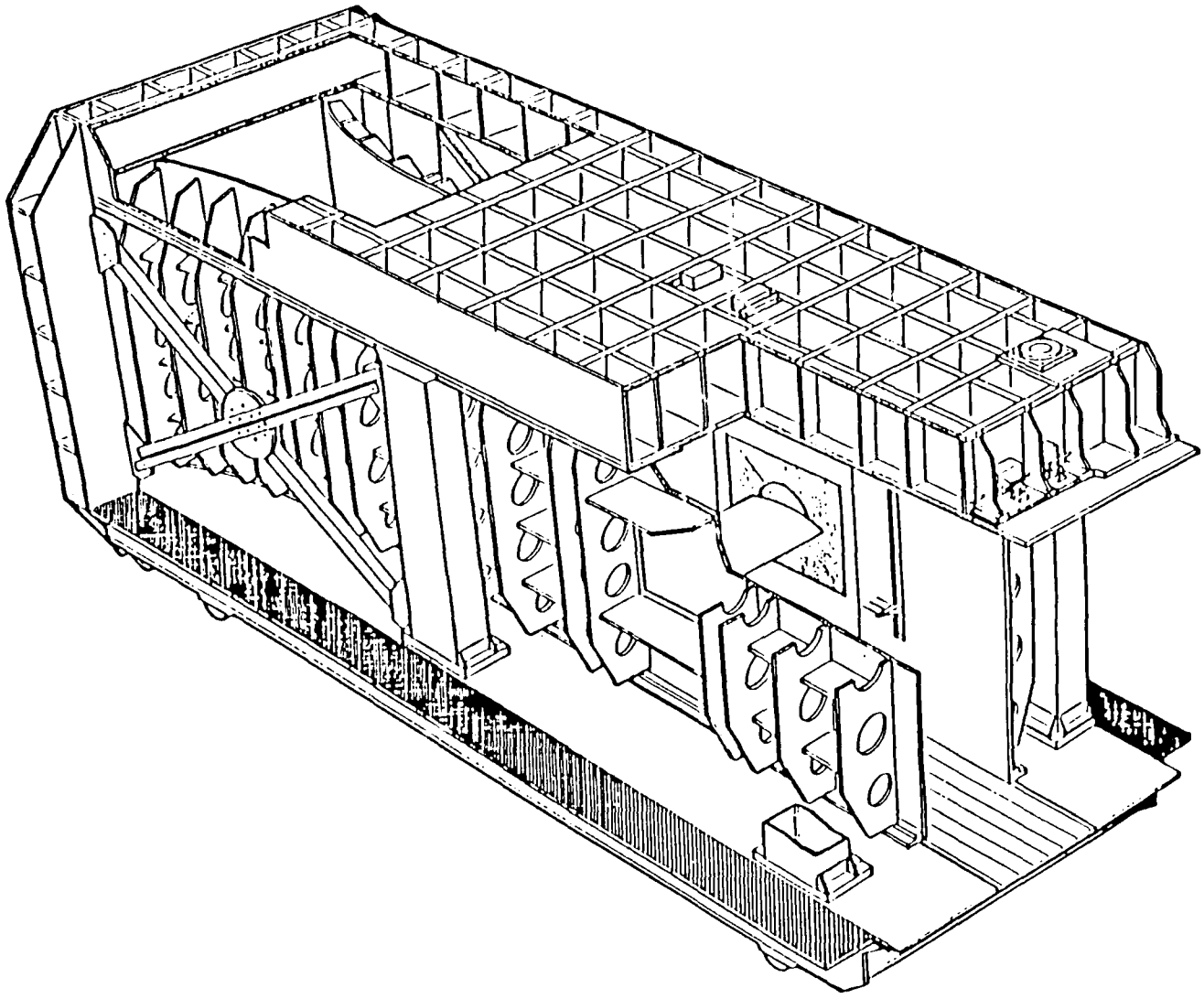

FIG. 3: 15-IN X 60-IN 2D TEST SECTION

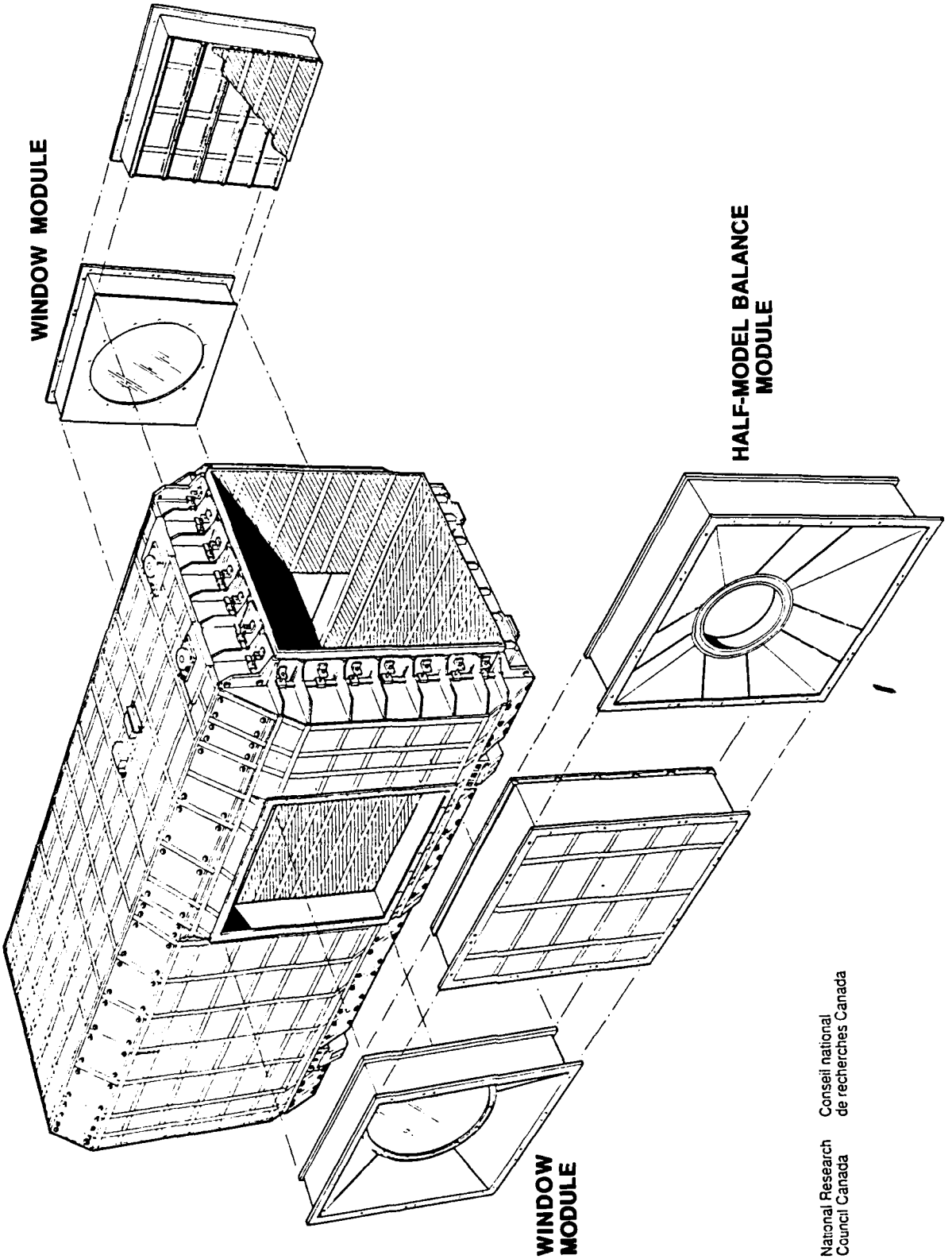

FIG. 4: 5-FT X 5-FT 3D TEST SECTION

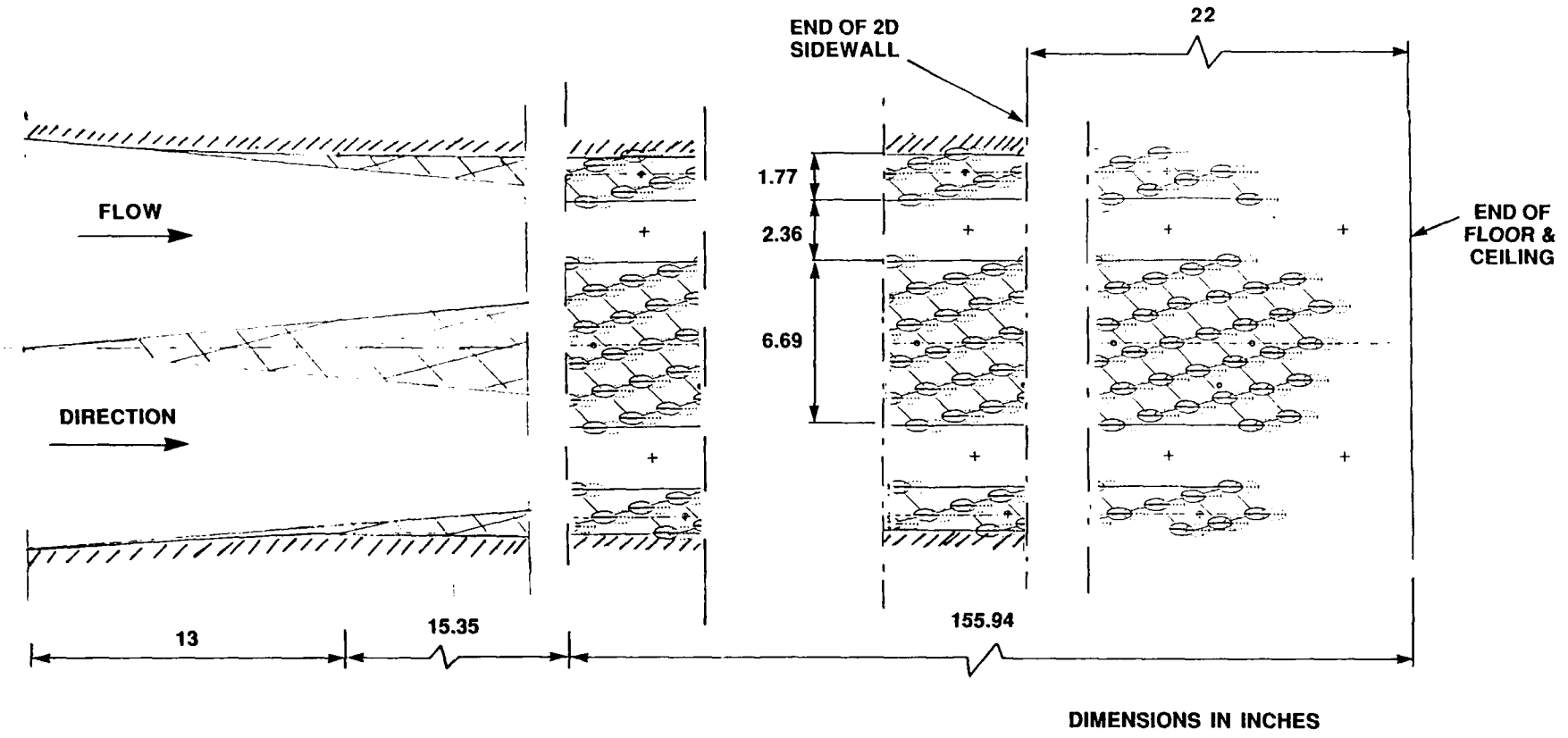

FIG. 5: PERFORATED WALL HOLE PATTERN: 2D INSERT FLOOR AND CEILING
(3D WALLS HAVE FIVE 6.69 IN WIDE PERFORATED STRIPS AND TWO 5.71 IN WIDE END STRIPS)

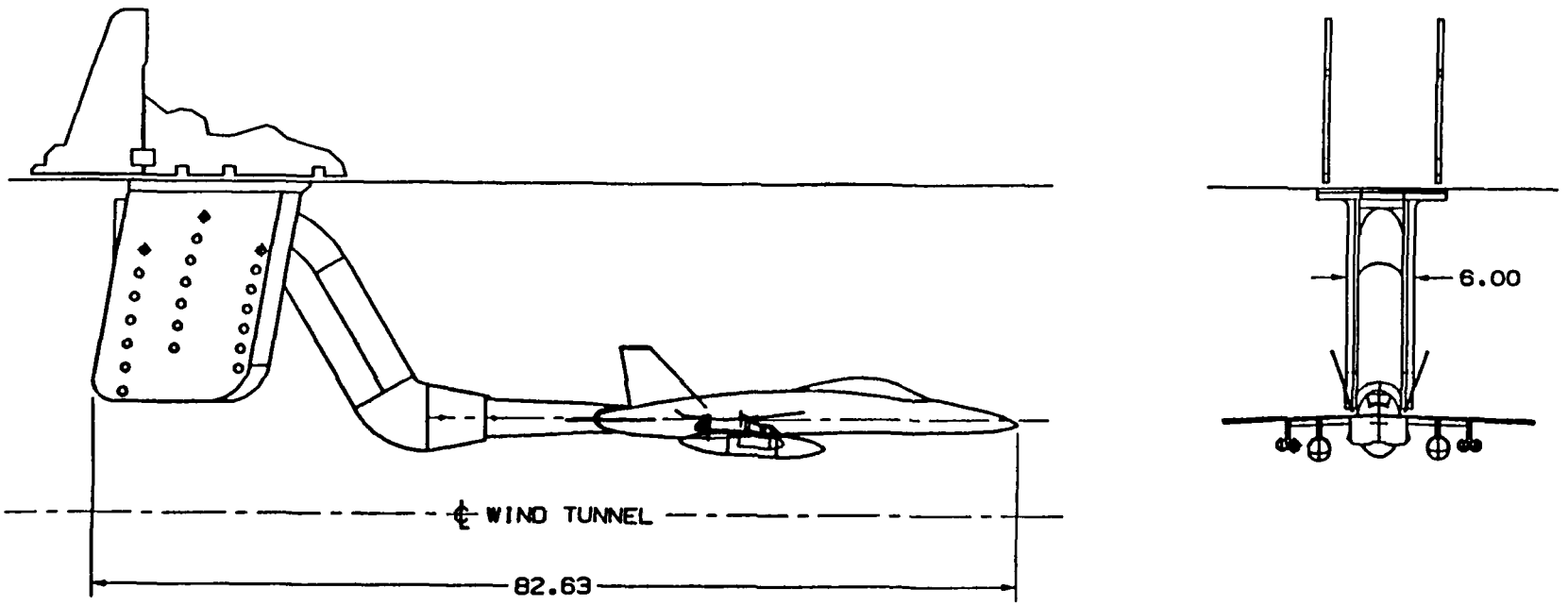

FIG. 6: ROOF MOUNTED STING

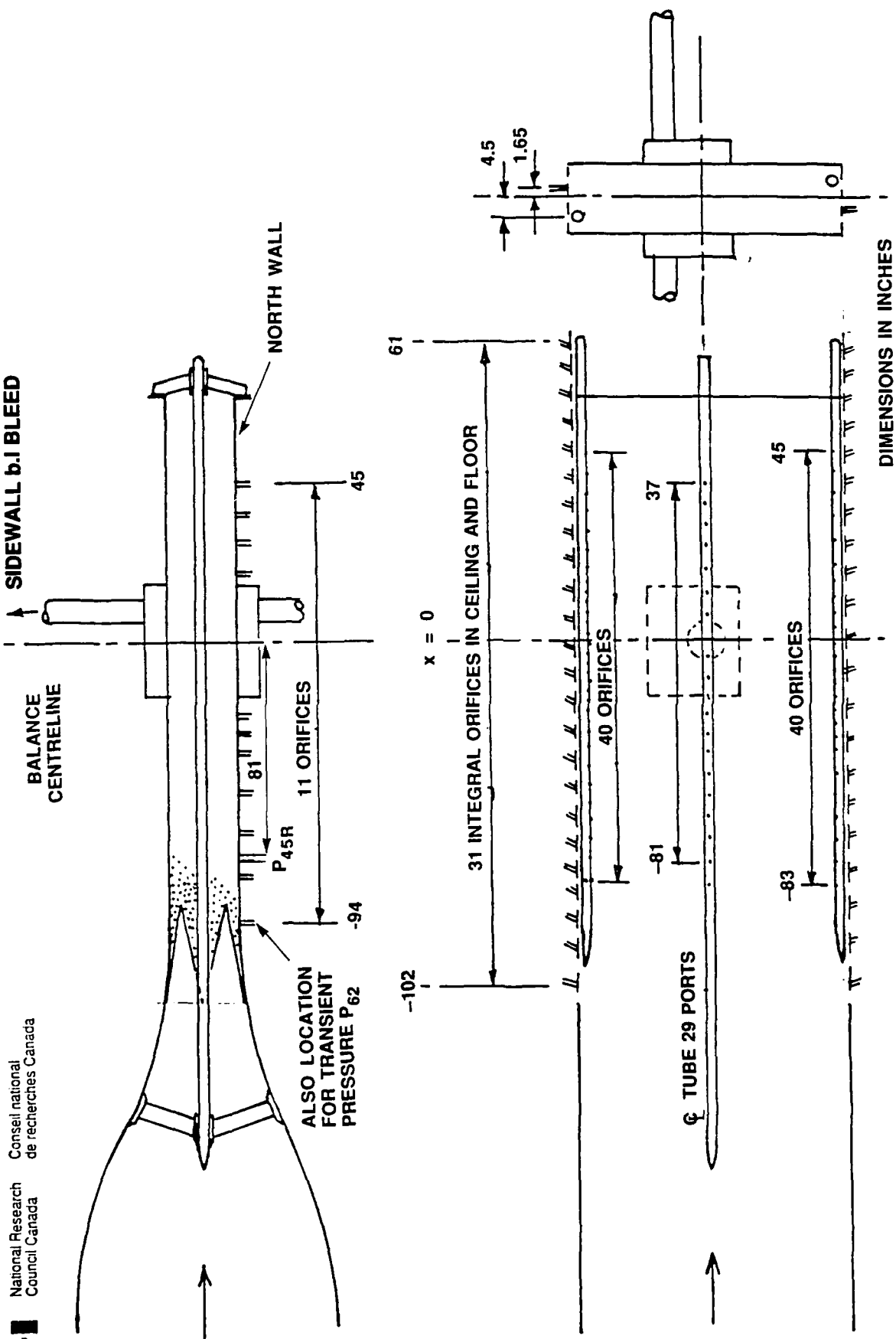

FIG. 7: 2D TEST SECTION STATIC PRESSURE CALIBRATION ARRANGEMENTS

National Research Council Canada | Conseil national de recherches Canada

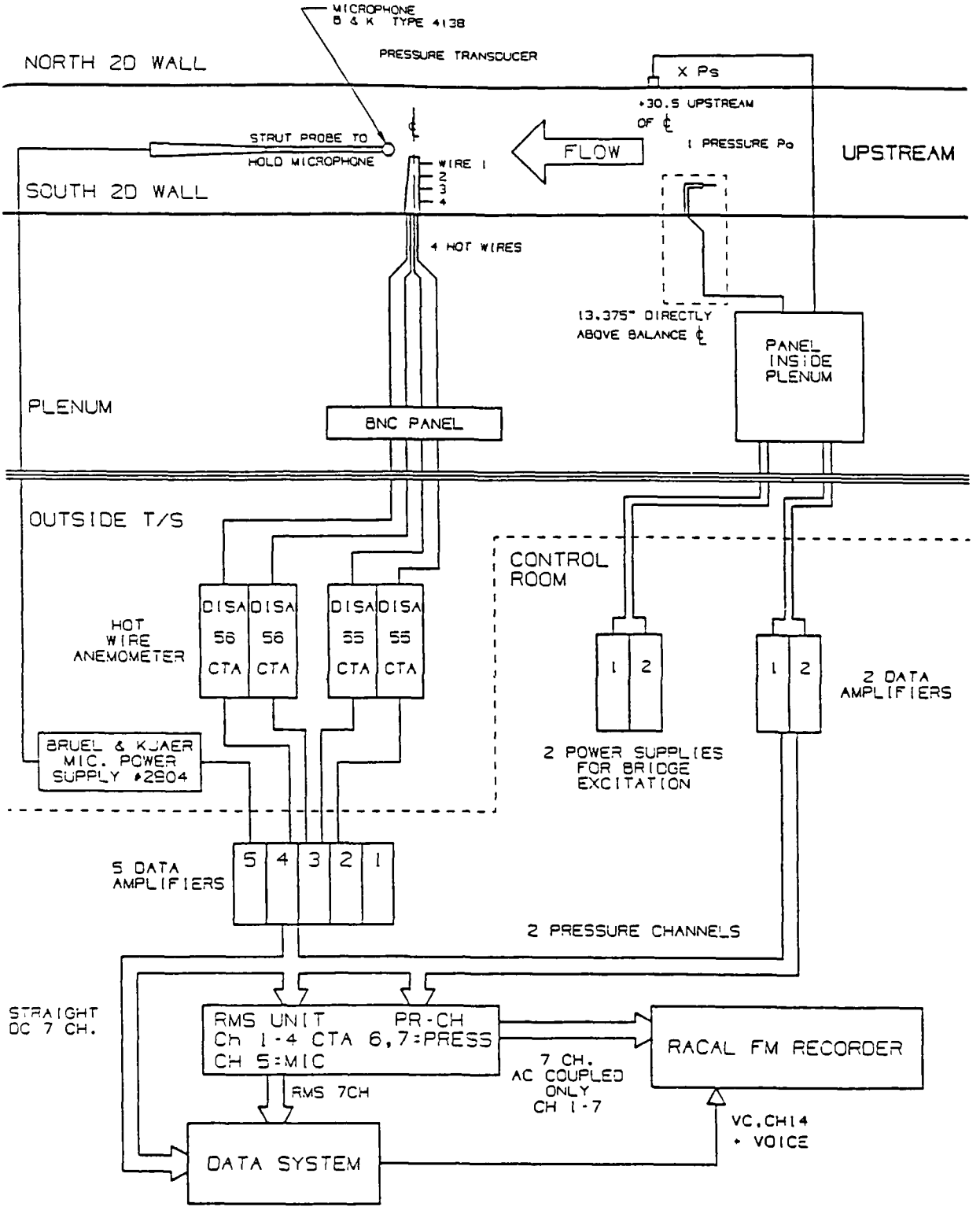

FIG. 8: FLOW QUALITY MEASURING SYSTEM

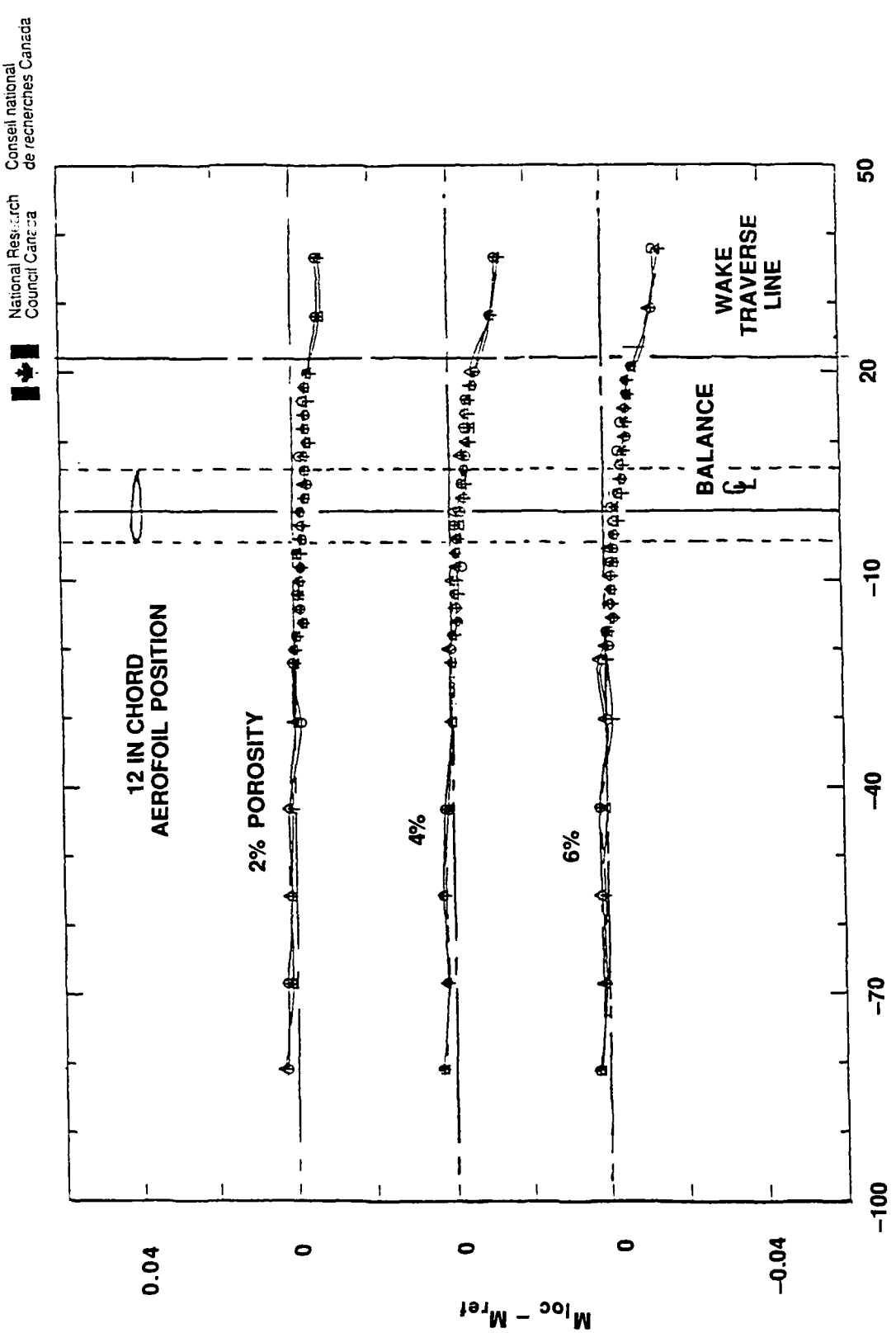

FIG. 9a: CENTRELINE MACH NUMBER DISTRIBUTION, M_{nom} = 0.4, Re = 15 x 10^6 ft^{-1}

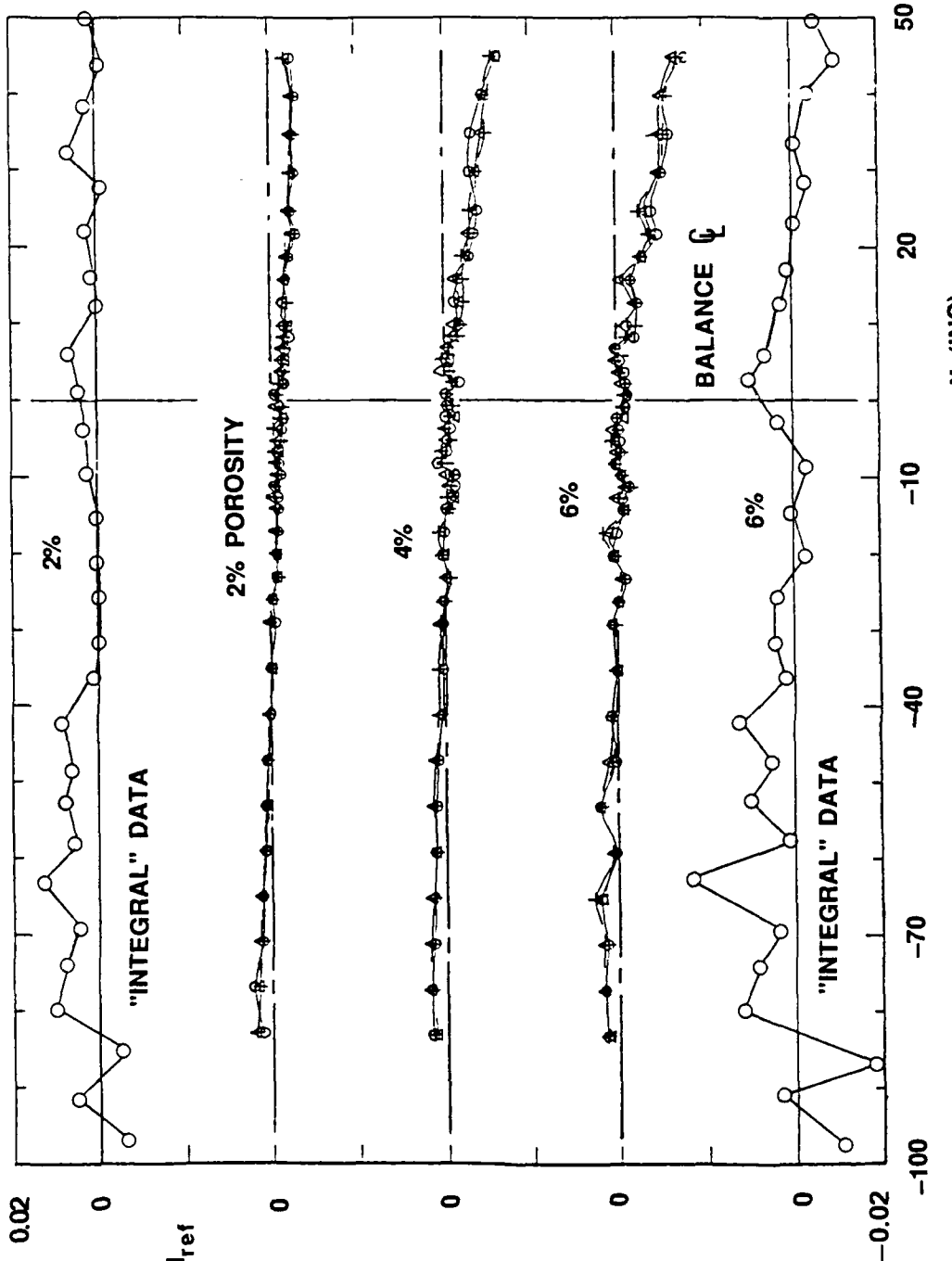

FIG. 9b: CEILING STATIC TUBE AND INTEGRAL ORIFICES MACH NUMBER DISTRIBUTION, M_{nom} = 0.4, Re = 15 x 10^6 ft^{-1}

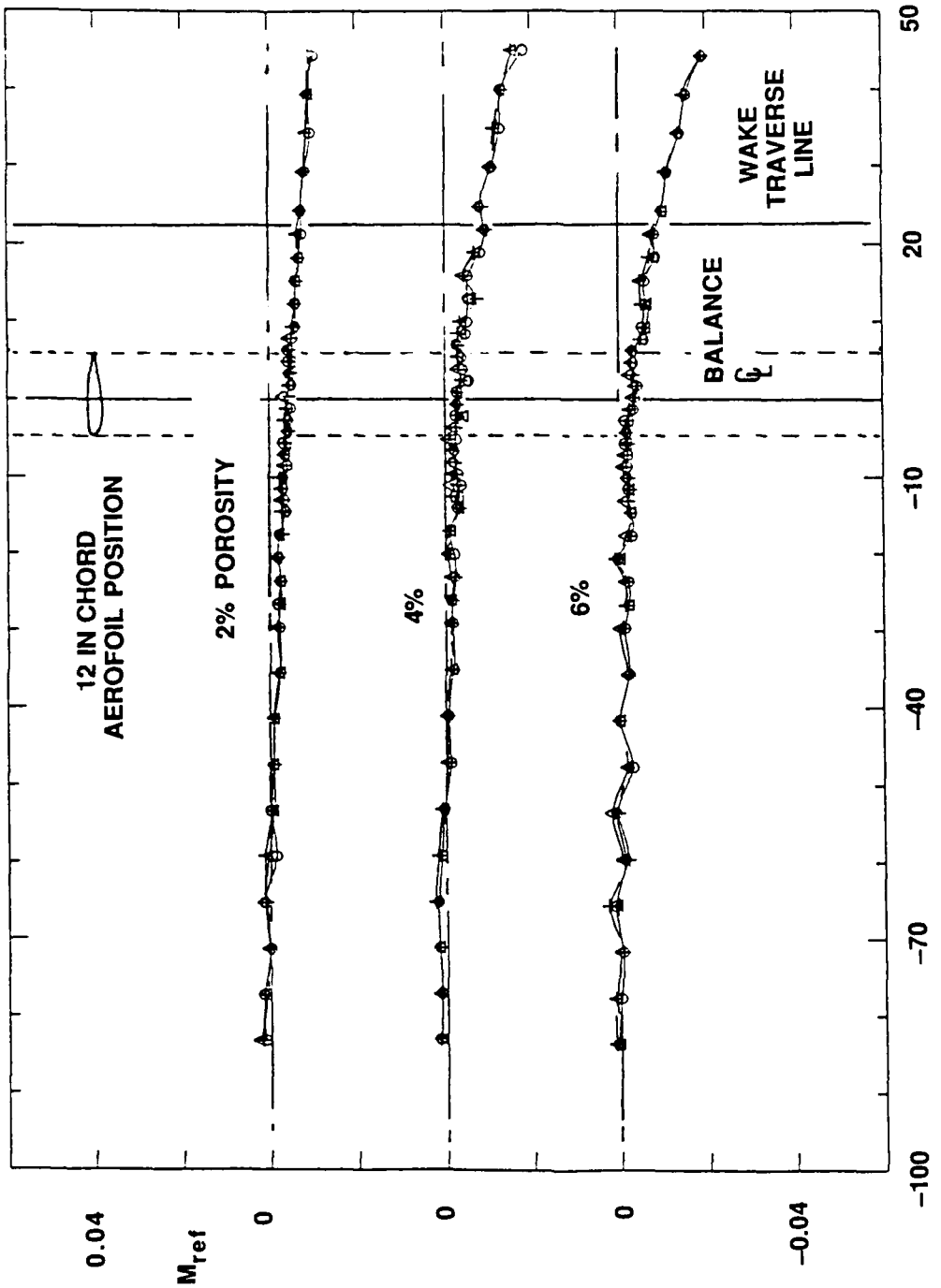

FIG. 9c: FLOOR STATIC TUBE MACH NUMBER DISTRIBUTION, M_{nom} = 0.4, Re = 15 x 10^6 ft^{-1}

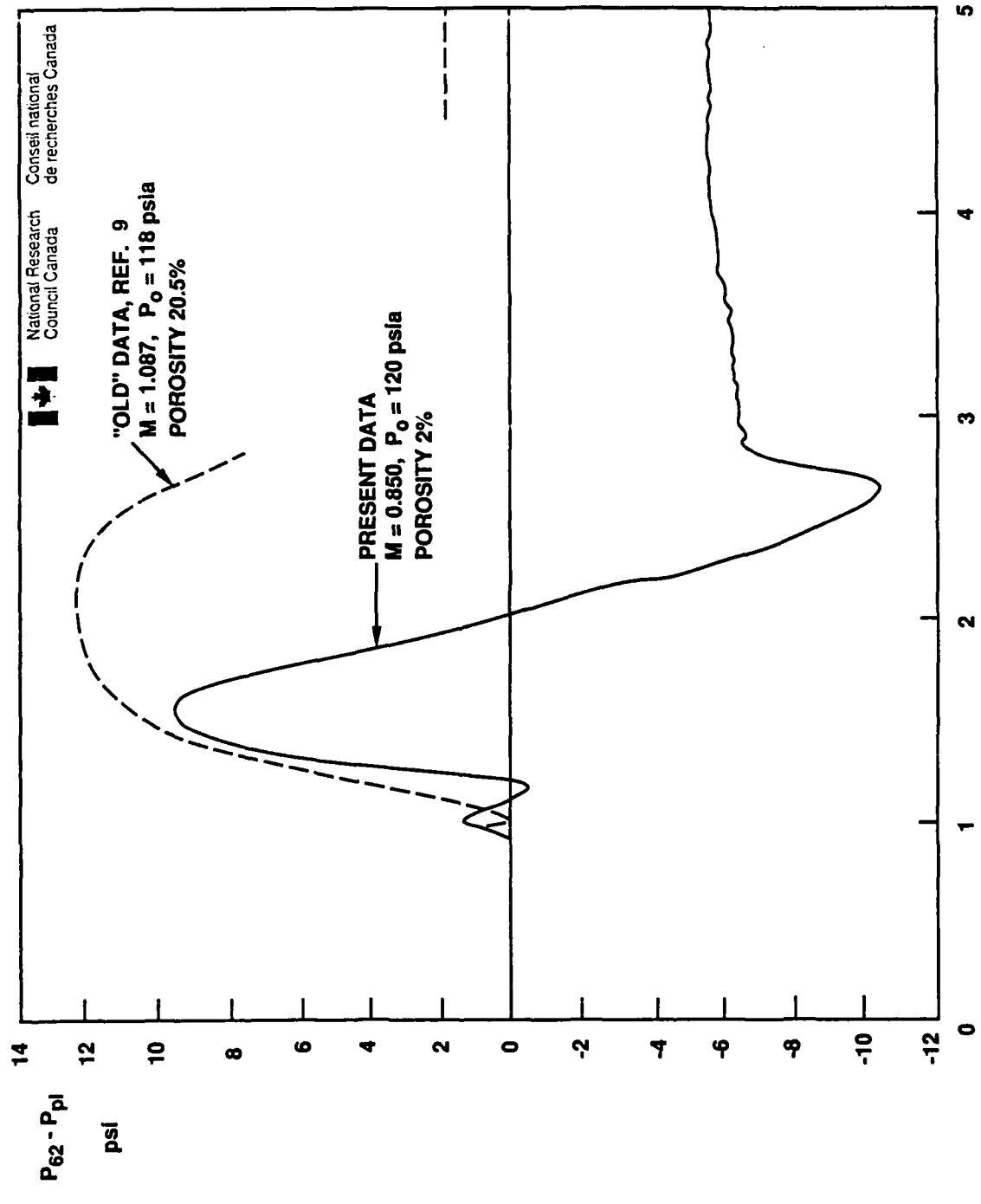

FIG. 10: TRANSIENT WALL PRESSURE SIGNATURES

National Research Council Canada
Conseil national de recherches Canada

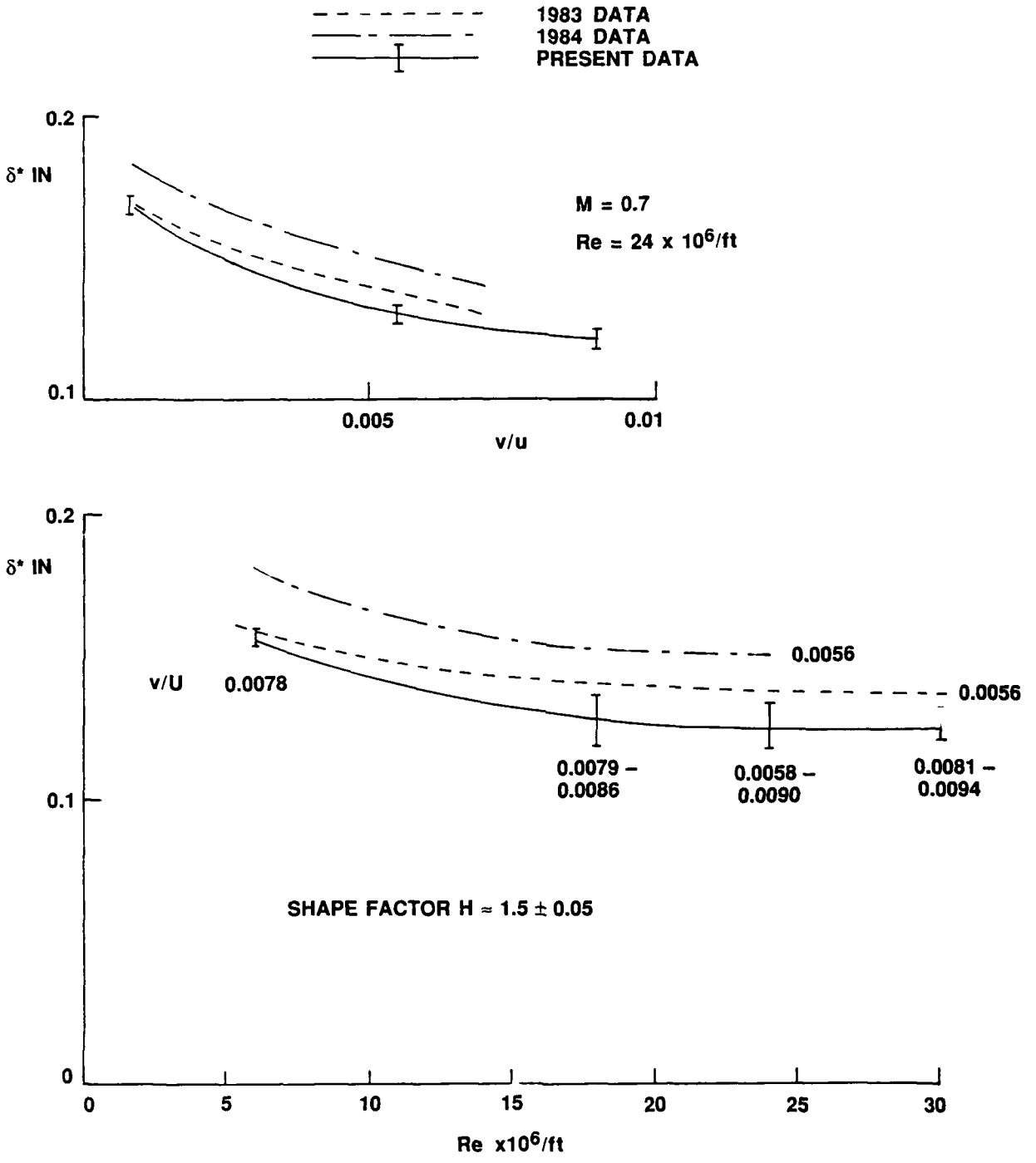

FIG. 11: SIDEWALL BOUNDARY LAYER CHARACTERISTICS

$$\left(\frac{\tilde{u}}{\bar{u}}\right)^2_{rms} = \frac{\left(\frac{\tilde{\rho u}}{\bar{\rho u}}\right)^2_{rms} + \left(\frac{\tilde{P}}{\bar{P}}\right)^2}{\left(1+(\gamma-1)M^2\right)^2}$$

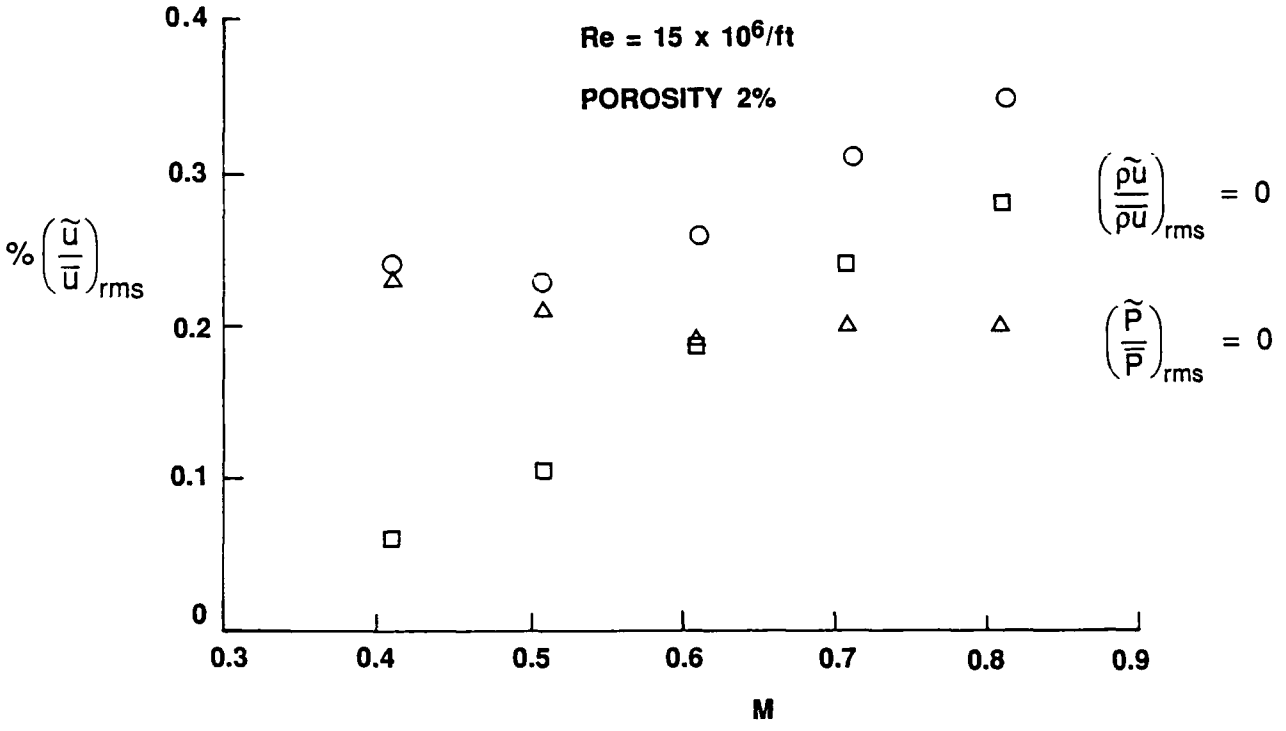

FIG. 12: 2D TEST SECTION TURBULENCE RESULTS

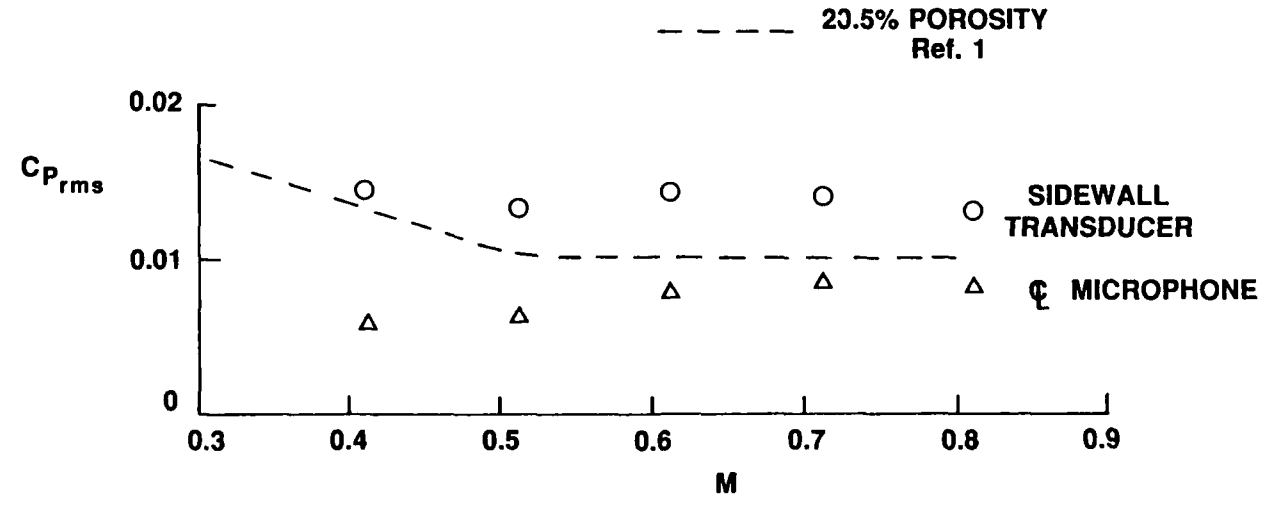

FIG. 13: CENTRELINE AND SIDEWALL STATIC PRESSURE FLUCTUATIONS, POROSITY 2%, Re = 15 x 10^6 ft^{-1}

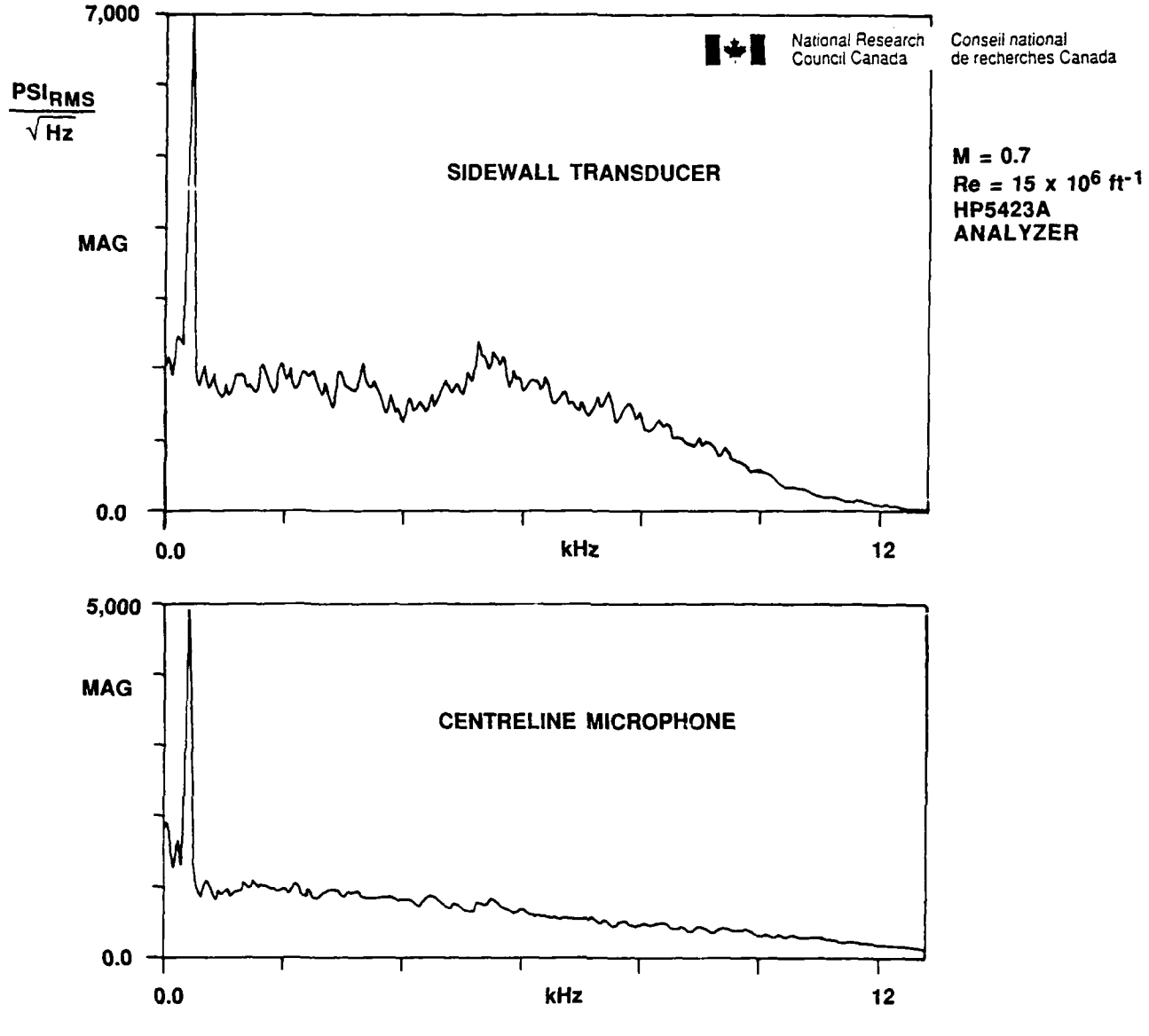

(a) NEW TEST SECTION, 2% POROSITY

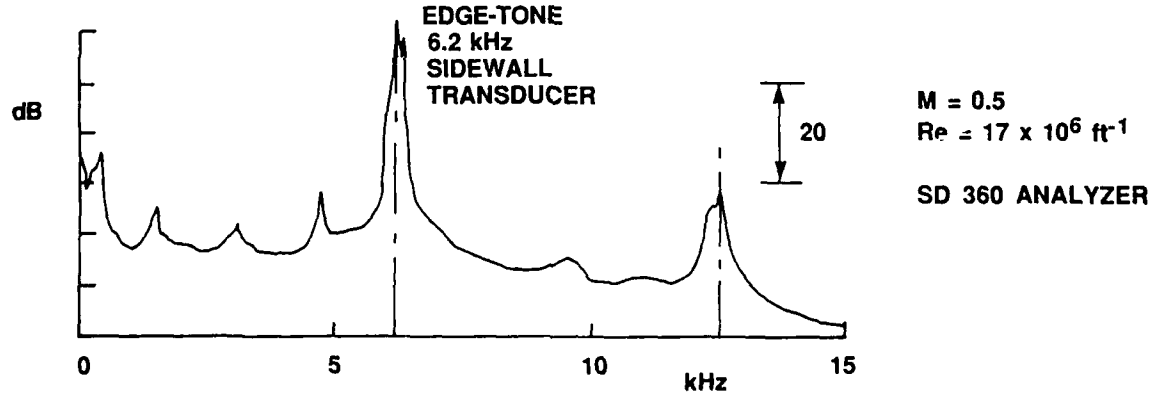

(b) 'OLD' TEST SECTION, 20.5% POROSITY (NORMAL HOLES)

FIG. 14: POWER SPECTRAL DENSITIES, 2D TEST SECTION

National Research Council Canada | Conseil national de recherches Canada

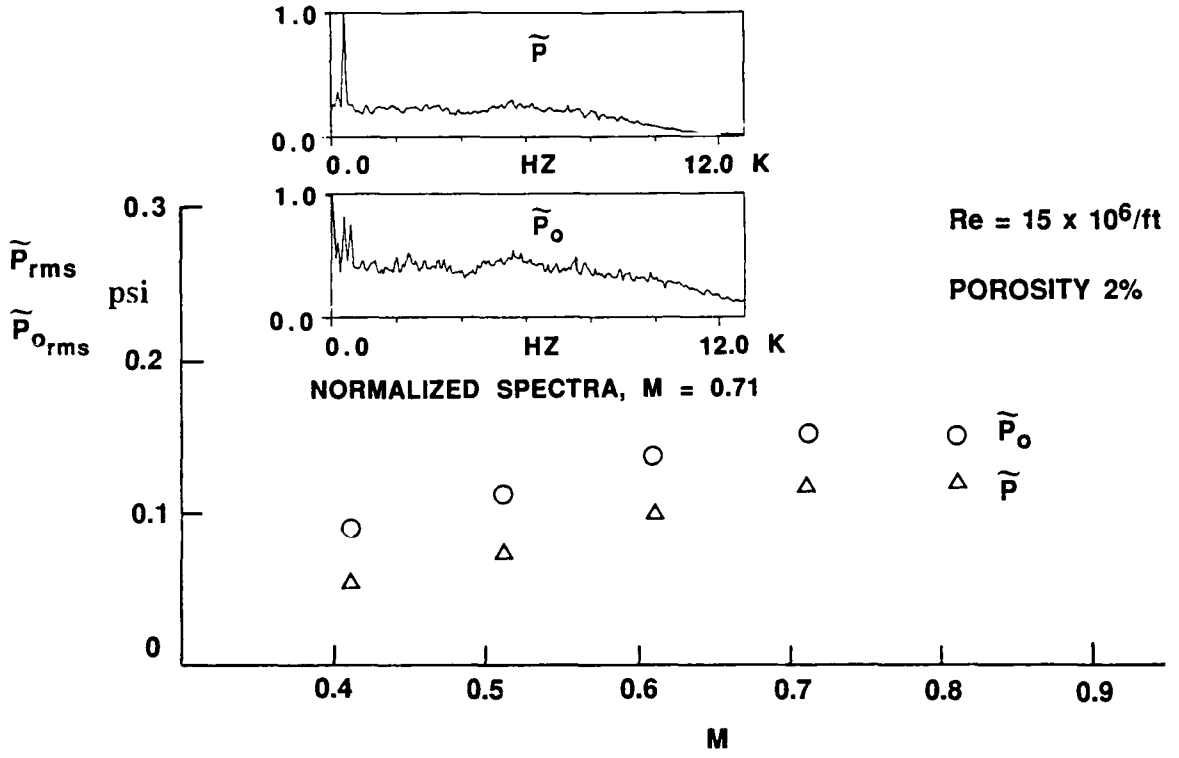

FIG. 15: ABSOLUTE LEVEL OF 2D TEST SECTION STATIC AND TOTAL PRESSURE FLUCTUATIONS

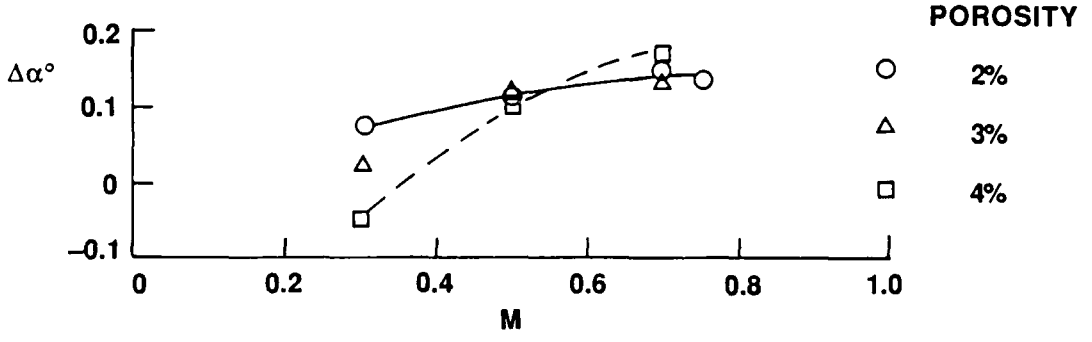

FIG. 16: 2D TEST SECTION FLOW ANGULARITY

National Research Council Canada
Conseil national de recherches Canada

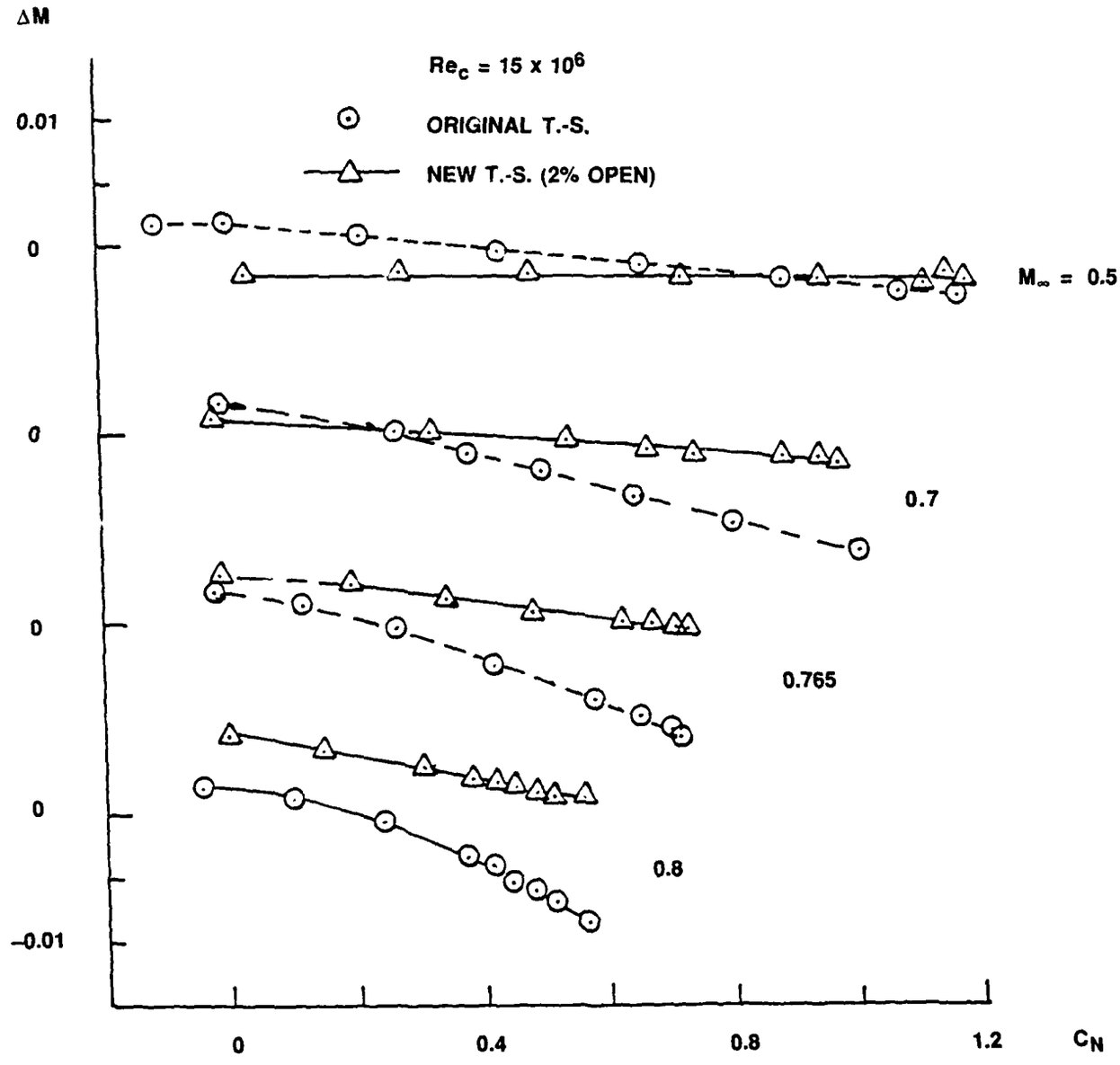

FIG. 17: WALL INDUCED MACH NUMBER CORRECTIONS FOR 9" CHORD AIRFOIL

National Research Council Canada | Conseil national de recherches Canada

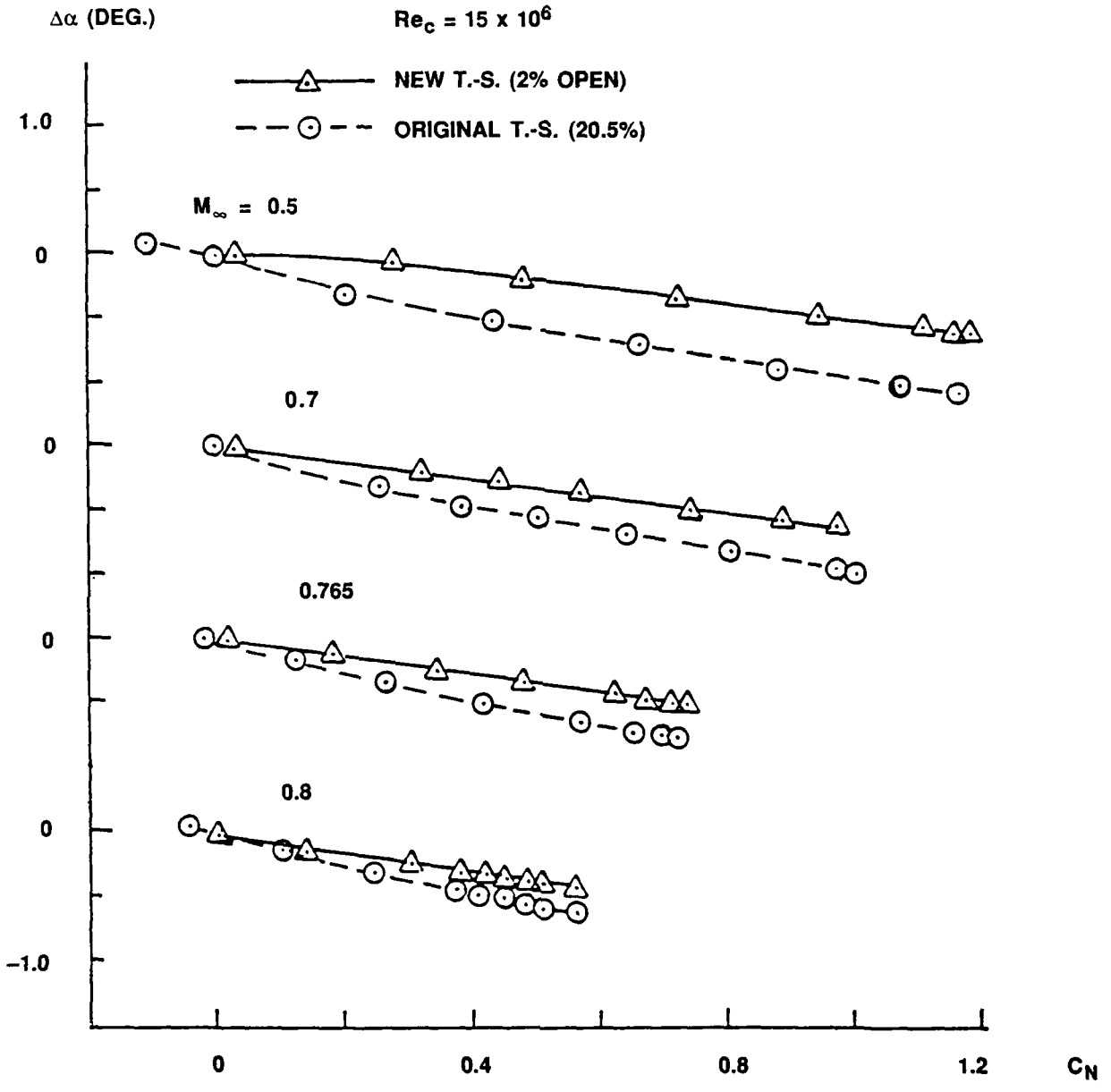

FIG. 18: WALL INDUCED ANGLE OF ATTACK CORRECTIONS FOR 9" CHORD AIRFOIL

National Research Council Canada | Conseil national de recherches Canada

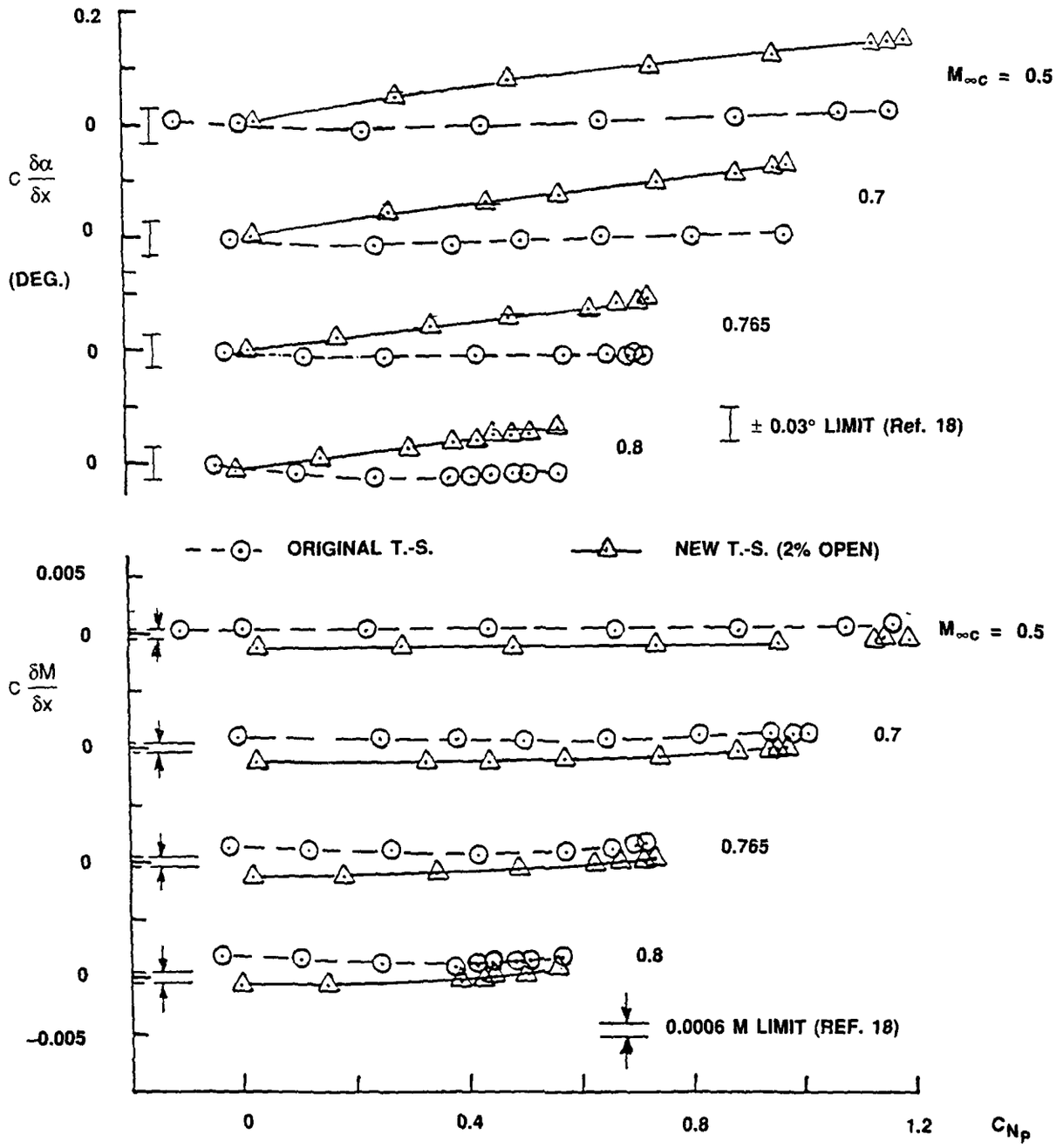

FIG. 19: WALL INDUCED STREAMWISE MACH NUMBER AND ANGLE OF ATTACK GRADIENTS FOR 9" CHORD AIRFOIL

National Research Council Canada | Conseil national de recherches Canada

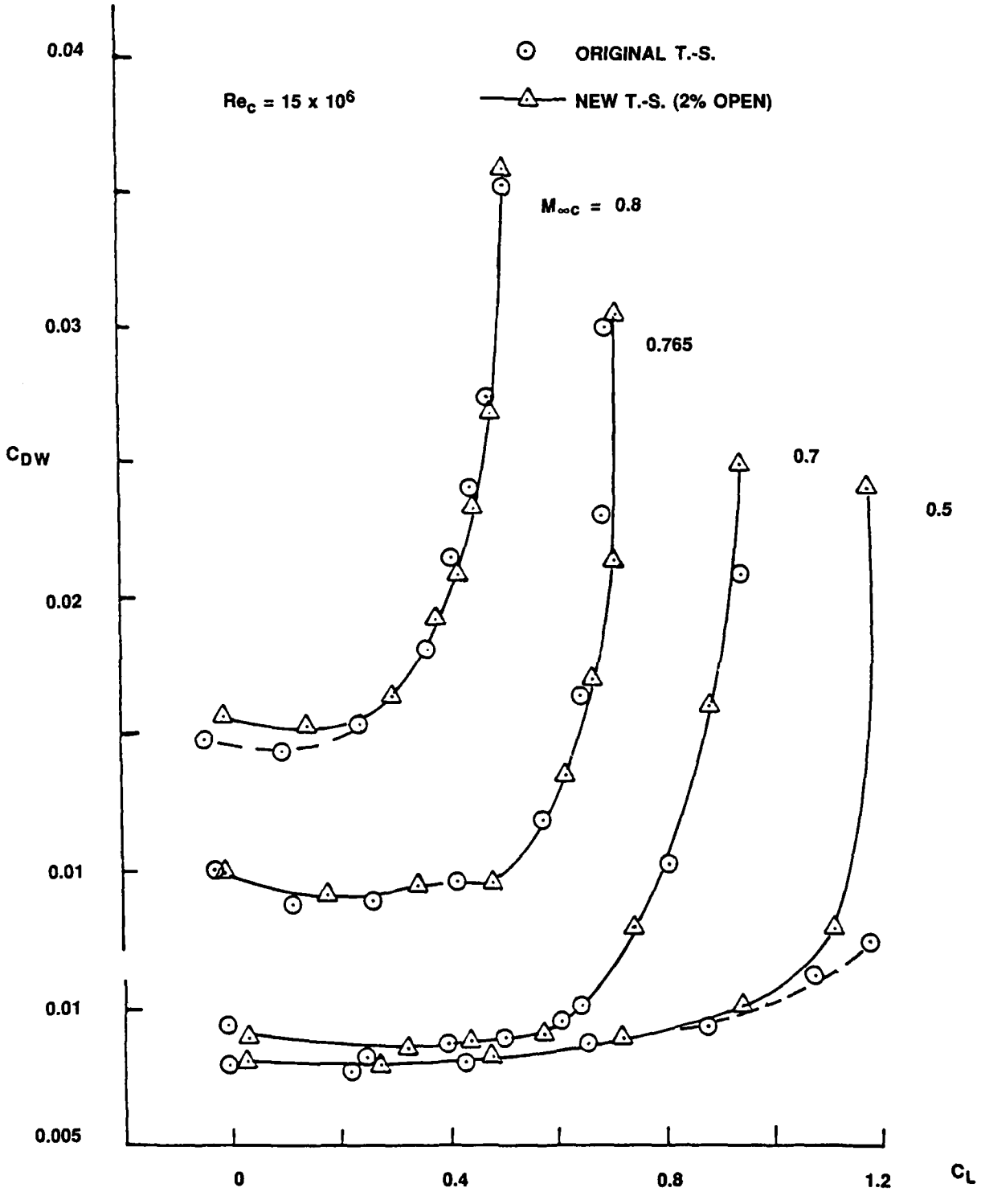

FIG. 20: DRAG-LIFT POLARS FOR 9" CHORD AIRFOIL

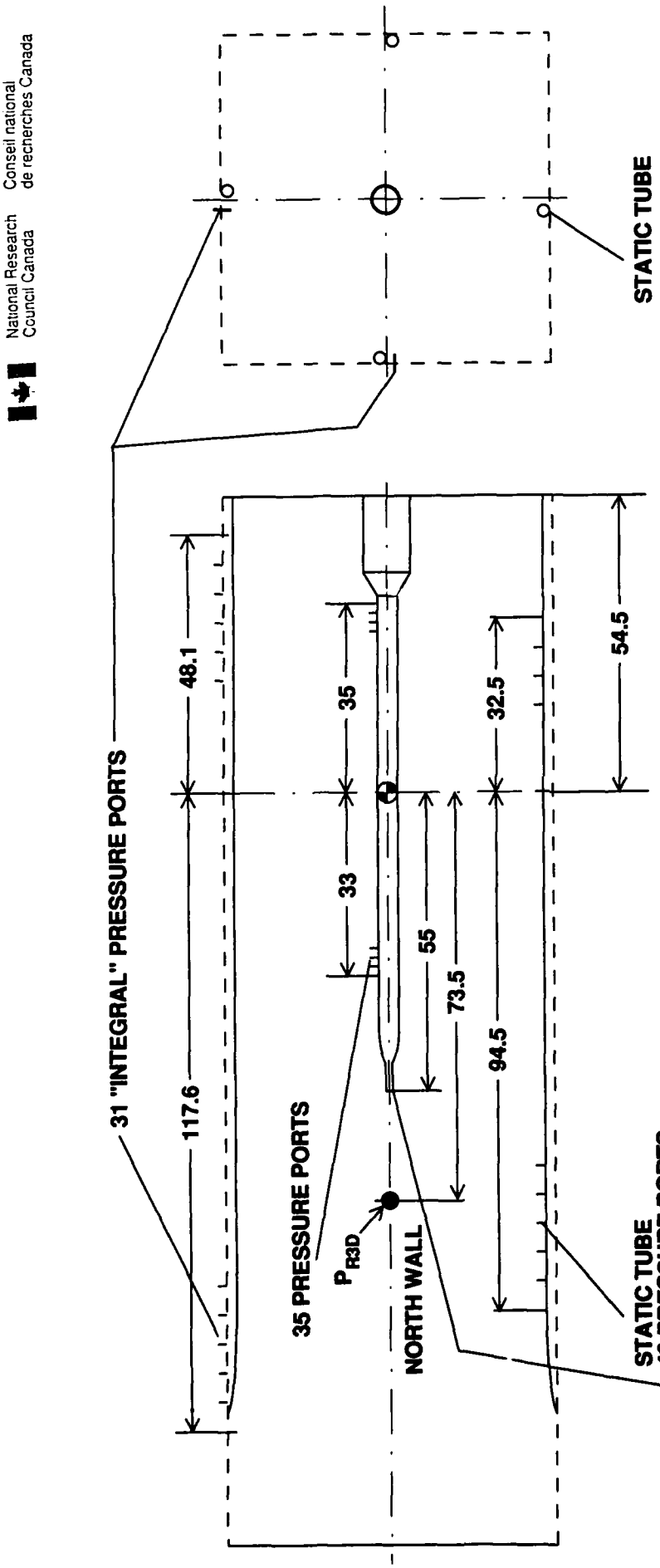

FIG. 21: ARRANGEMENT FOR CALIBRATION OF 3-D TEST SECTION

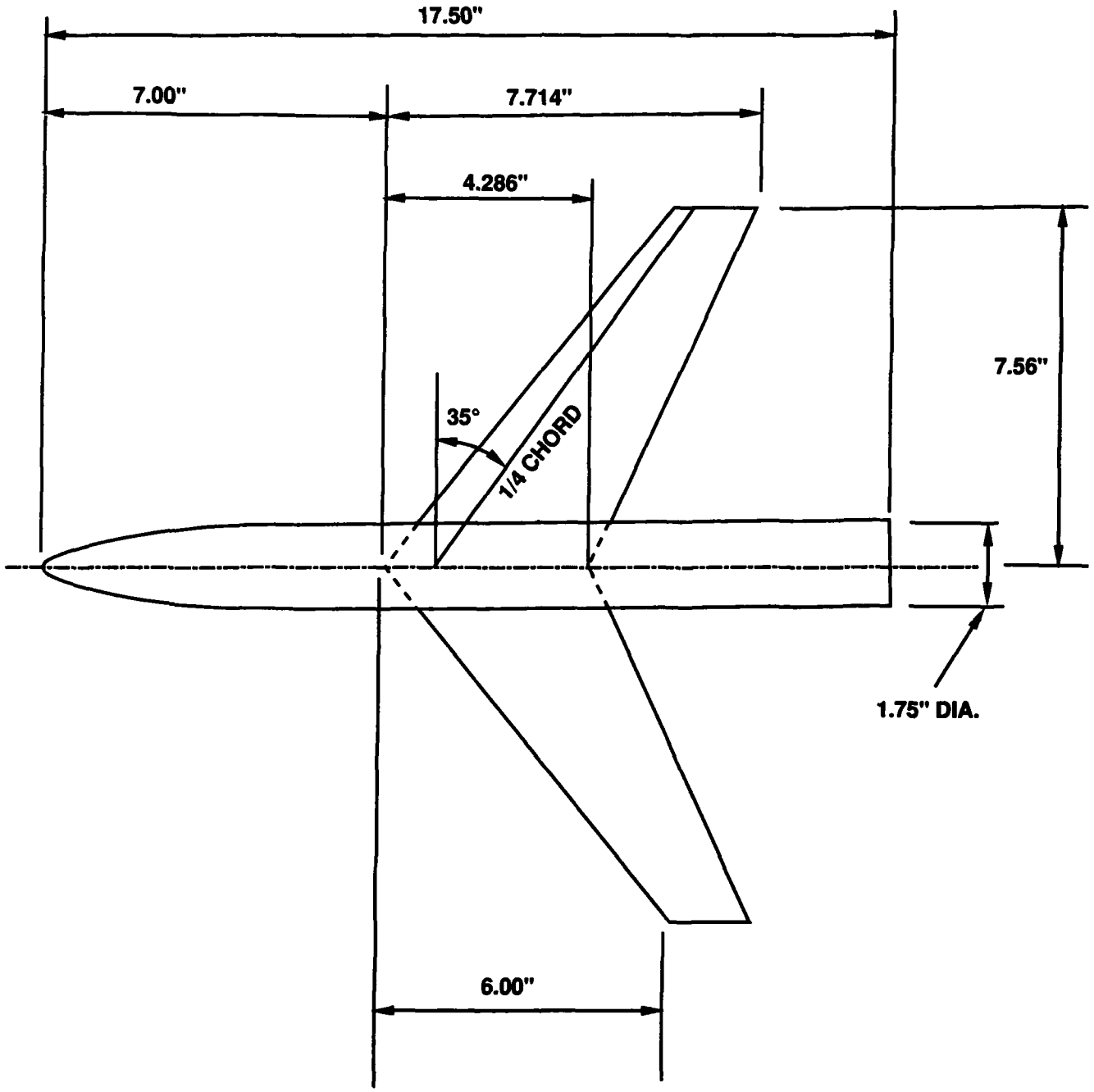

FIG. 22: SWEPT WING MODEL WBSC

National Research Council Canada | Conseil national de recherches Canada

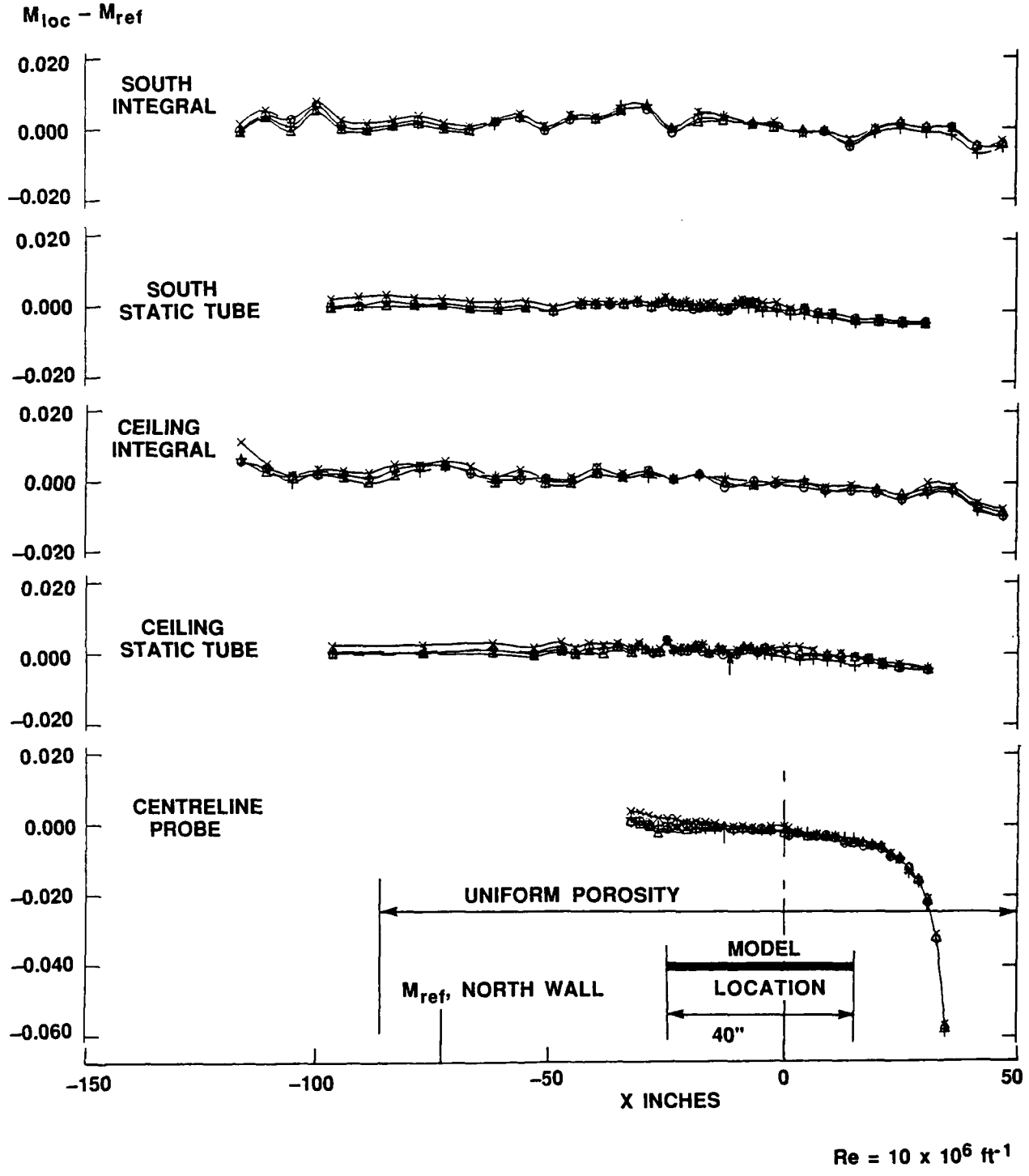

FIG. 23: MACH NUMBER DISTRIBUTION, M_{nom} = 0.5, 3D TEST SECTION

National Research Council Canada
Conseil national de recherches Canada

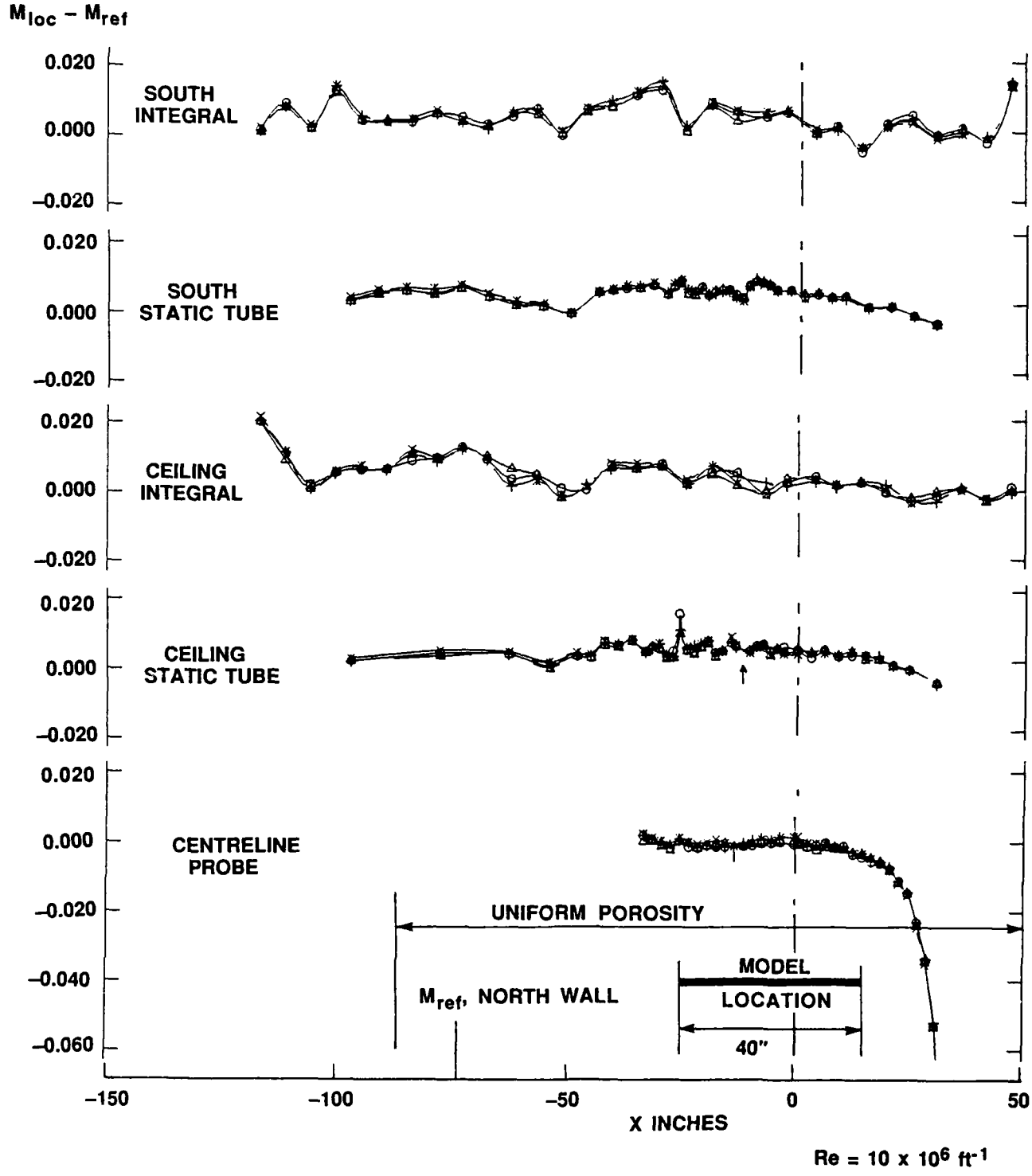

FIG. 24: MACH NUMBER DISTRIBUTION, M_{nom} = 0.9, 3D TEST SECTION

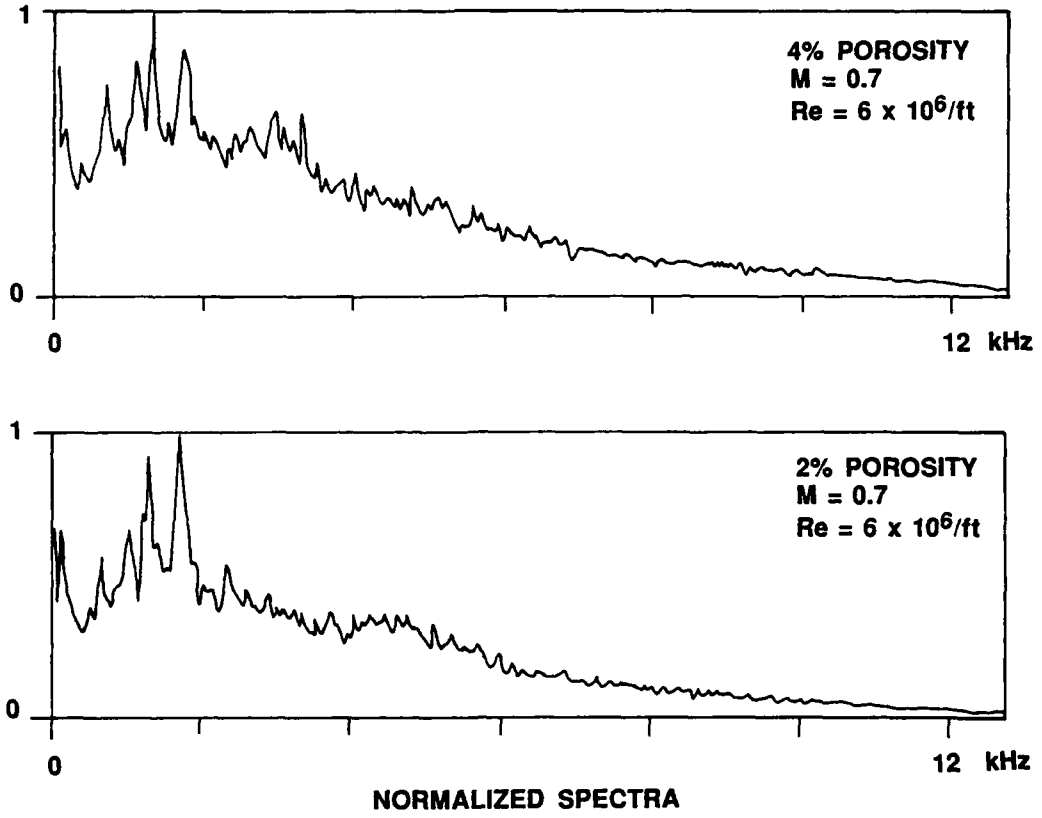

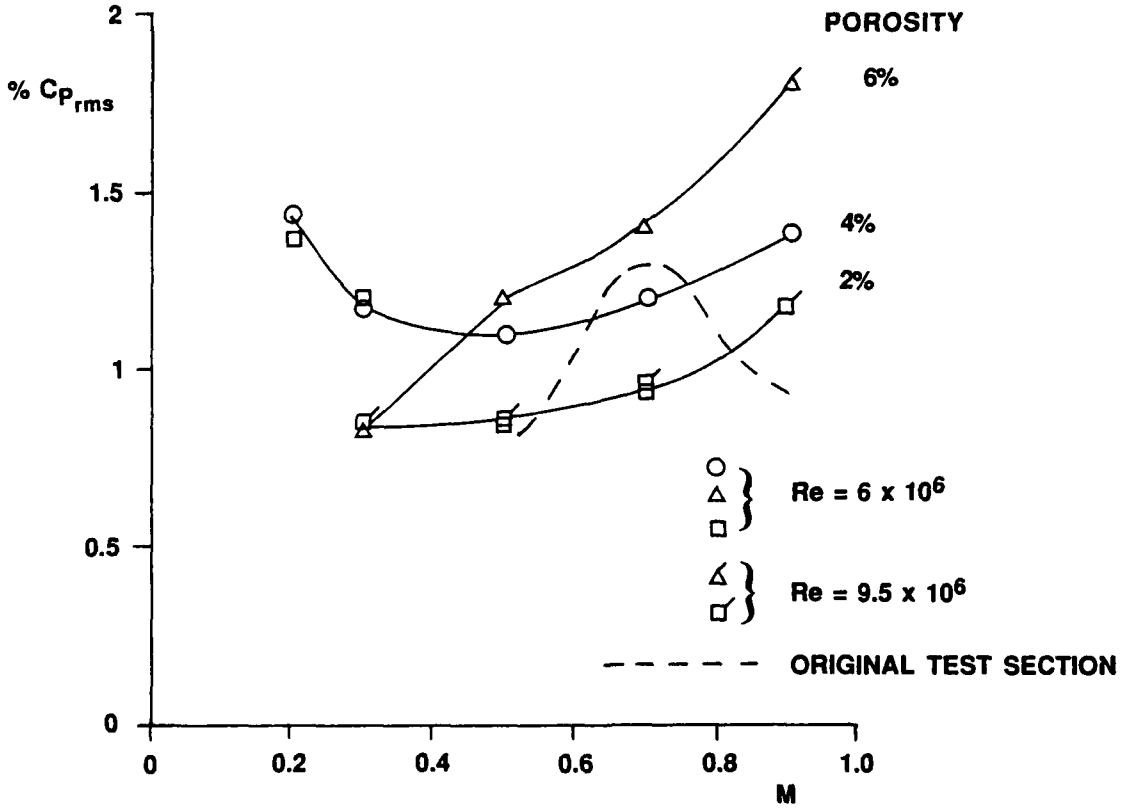

FIG. 25: CENTRELINE STATIC PRESSURE FLUCTUATIONS AND SAMPLE POWER SPECTRA, 3D TEST SECTION

National Research Council Canada | Conseil national de recherches Canada

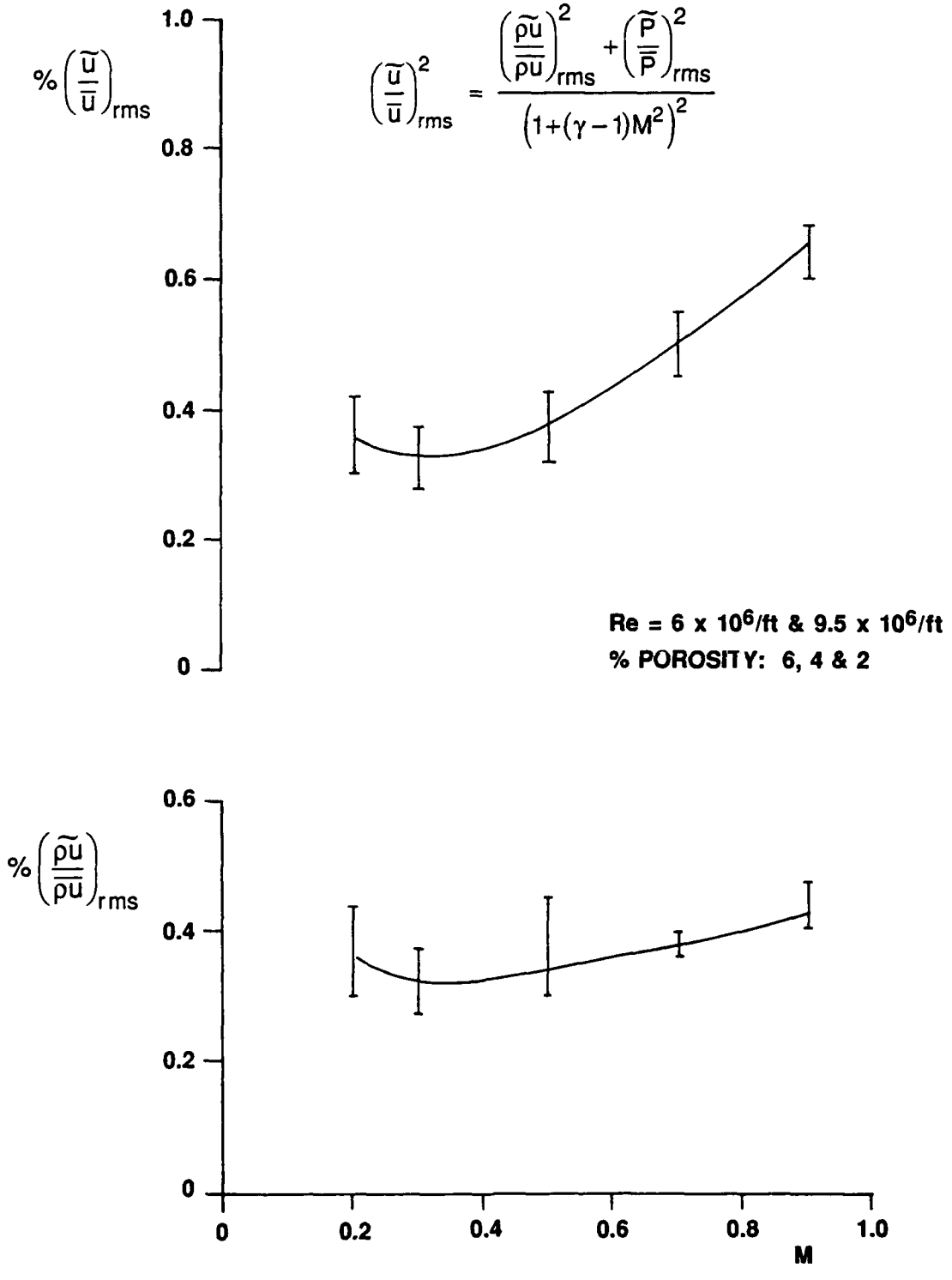

FIG. 26: CENTRELINE MASS FLUX AND VELOCITY FLUCTUATIONS, 3D TEST SECTION

National Research Council Canada
Conseil national de recherches Canada

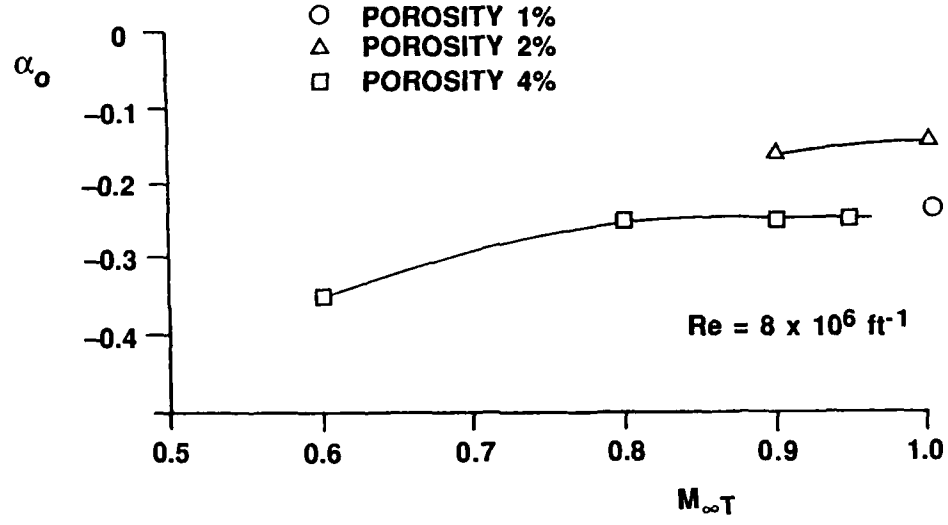

FIG. 27: 3D TEST SECTION FLOW ANGULARITY

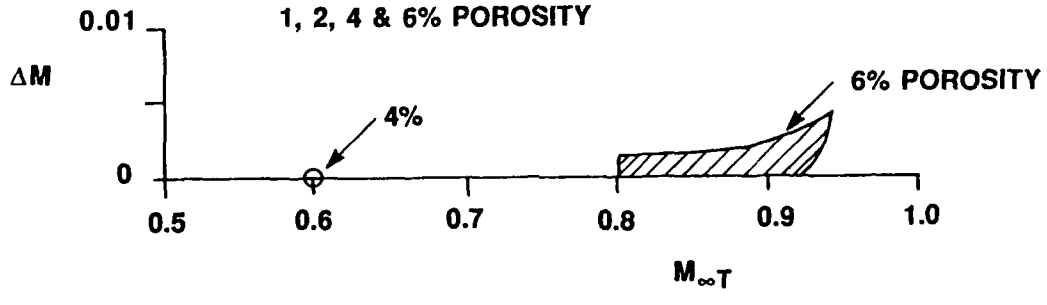

FIG. 28: WALL INDUCED MACH NUMBER CORRECTION FOR 0.1% BLOCKAGE MODEL WBSC

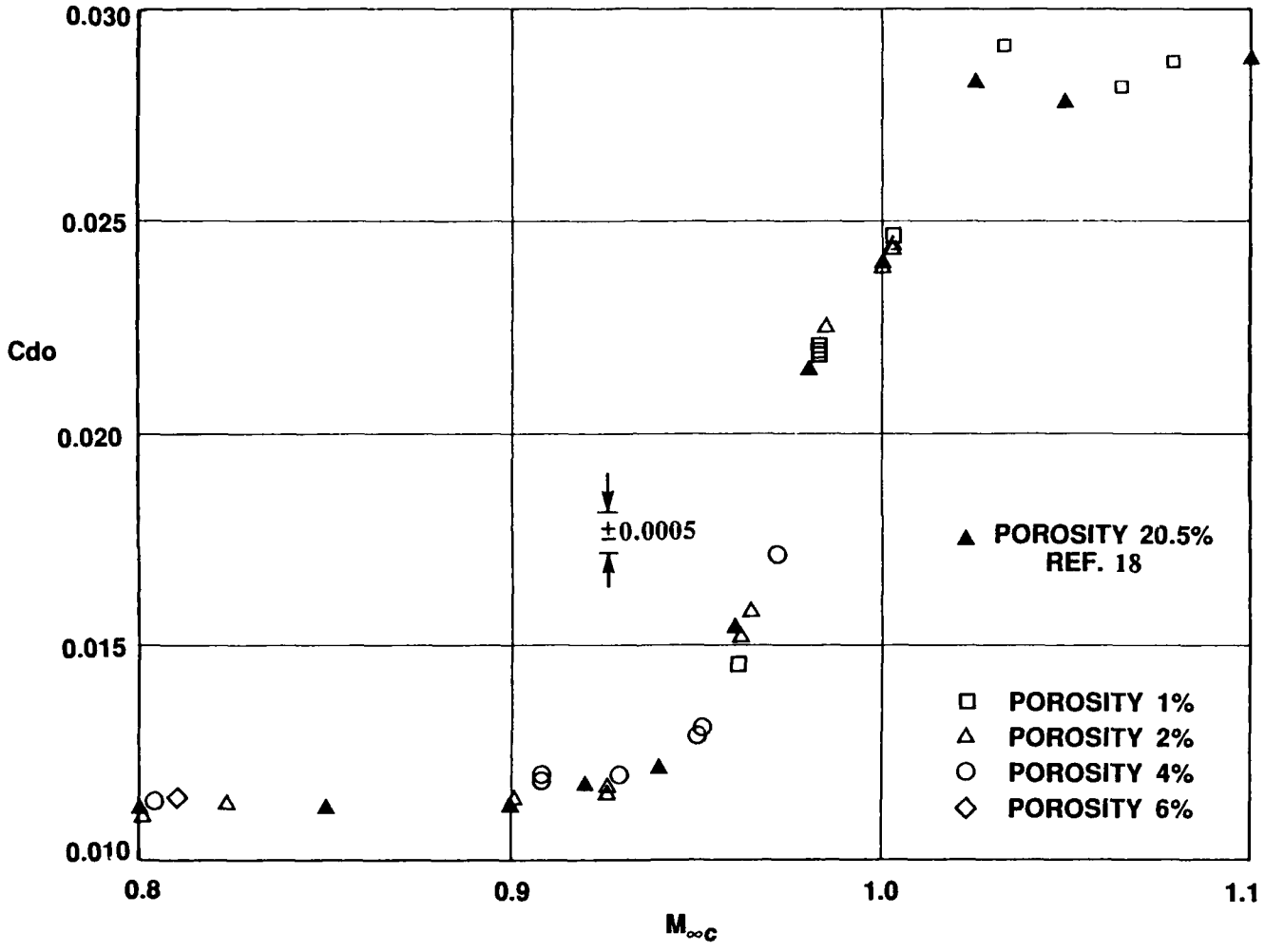

FIG. 29: ZERO LIFT DRAG COEFFICIENT RESULTS FOR MODEL WBSC

REPORT DOCUMENTATION PAGE / PAGE DE DOCUMENTATION DE RAPPORT

REPORT/RAPPORT	REPORT/RAPPORT
NAE-AN-62 (1a)	NRC No. 31216 (1b)
REPORT SECURITY CLASSIFICATION / CLASSIFICATION DE SÉCURITÉ DE RAPPORT: Unclassified (2)	DISTRIBUTION (LIMITATIONS): Unlimited (3)

TITLE/SUBTITLE/TITRE/SOUS-TITRE (4)

New Transonic Test Sections for the NAE 5Ftx5Ft Trisonic Wind Tunnel

AUTHOR(S)/AUTEUR(S) (5)

L.H. Ohman, D. Brown, Y.Y. Chan, R.D. Galway, S.M. Hashim, M. Khalid, A. Malek, M. Mokry, N. Tang, J. Thain

SERIES/SÉRIE (6)

Aeronautical Note

CORPORATE AUTHOR/PERFORMING AGENCY/AUTEUR D'ENTREPRISE/AGENCE D'EXÉCUTION (7)

National Research Council Canada
National Aeronautical Establishment
High Speed Aerodynamics Laboratory

SPONSORING AGENCY/AGENCE DE SUBVENTION (8)

DATE (9)	FILE/DOSSIER (10)	LAB. ORDER / COMMANDE DU LAB. (11)	PAGES (12a)	FIGS/DIAGRAMMES (12b)
90-01			66	29

NOTES (13)

DESCRIPTORS (KEY WORDS)/MOTS-CLÉS (14)

1. Trisonic wind tunnels
2. Wind tunnels (blowdown)
3. Wind tunnels — Canada (NAE)

SUMMARY/SOMMAIRE (15)

The NAE 5ftx5ft blowdown wind tunnel has undergone a major upgrade of its transonic testing capabilities. Two entirely new test sections, one for testing two-dimensional models (2D) and one for testing three-dimensional models and reflection plane models (3D), have been constructed The two test sections are parts of the so-called Roll-in Roll-out Test Section System, so designed that an interchange between the two sections can be carried out within two days, a process that previously required about three weeks. The new test sections have, as before, perforated walls, but with different hole geometry, viz. slanted holes with splitter plates as opposed to normal holes in the original test sections. The design and manufacturing was carried out by Canadian companies.

The two test sections have been calibrated with regard to pressure distributions, flow quality (turbulence and pressure fluctuations), side wall boundary layer characteristics (2D), flow angularity and wall interference characteristics. Results from these investigations are presented and compared with corresponding data obtained in the original test sections.